



**HAL**  
open science

## Trophic ecology of a blooming jellyfish (*Aurelia coerulea*) in a Mediterranean coastal lagoon

Raquel Marques, Delphine Bonnet, Claire Carré, Cécile Roques, Audrey M. Darnaude

► **To cite this version:**

Raquel Marques, Delphine Bonnet, Claire Carré, Cécile Roques, Audrey M. Darnaude. Trophic ecology of a blooming jellyfish (*Aurelia coerulea*) in a Mediterranean coastal lagoon. *Limnology and Oceanography*, 2021, 66 (1), pp.141-157. 10.1002/lno.11593 . hal-03411044

**HAL Id: hal-03411044**

**<https://hal.umontpellier.fr/hal-03411044>**

Submitted on 17 Nov 2021

**HAL** is a multi-disciplinary open access archive for the deposit and dissemination of scientific research documents, whether they are published or not. The documents may come from teaching and research institutions in France or abroad, or from public or private research centers.

L'archive ouverte pluridisciplinaire **HAL**, est destinée au dépôt et à la diffusion de documents scientifiques de niveau recherche, publiés ou non, émanant des établissements d'enseignement et de recherche français ou étrangers, des laboratoires publics ou privés.

1 **Trophic ecology of a blooming jellyfish (*Aurelia coerulea*) in a**  
2 **Mediterranean coastal lagoon**

3  
4 *Raquel MARQUES<sup>1</sup>, Delphine BONNET<sup>1</sup>, Claire CARRÉ<sup>1</sup>, Cécile ROQUES<sup>1</sup>, Audrey M.*  
5 *DARNAUDE<sup>1</sup>*

6 <sup>1</sup> MARBEC, Univ. Montpellier, CNRS, Ifremer, IRD, Montpellier, France

7  
8  
9 **Corresponding author:**

10 [marques.rfs@gmail.com](mailto:marques.rfs@gmail.com) / [raquel.marques@umontpellier.fr](mailto:raquel.marques@umontpellier.fr)

11 CC093, Place Eugène Bataillon, 34095 Montpellier Cedex 05, France

12 Tel: +33769370312

13 **Co-authors contact:**

14 [delphine.bonnet@umontpellier.fr](mailto:delphine.bonnet@umontpellier.fr); [claire.carre@ird.fr](mailto:claire.carre@ird.fr); [Cecile.Roques@cnrs.fr](mailto:Cecile.Roques@cnrs.fr);

15 [Audrey.Darnaude@cnrs.fr](mailto:Audrey.Darnaude@cnrs.fr)

16  
17 **Running head:** Trophic ecology of jellyfish in a coastal lagoon

18 **Key words:** Stable Isotopes, Diet, Trophic niche, Trophic competition, Population dynamics,

19 Scyphistomae, Medusae, Oysters

20 **Abstract**

21 The current lack of knowledge on the trophic ecology of scyphozoans, particularly at the  
22 benthic stage, prevents a full understanding of the controls on many jellyfish blooms. The  
23 blooming scyphozoan (*Aurelia coerulea*) completes its entire life cycle in the Thau lagoon  
24 (southern France), where the annual population dynamics of both its benthic and pelagic  
25 stages have been described. This offered an exceptional framework to investigate the trophic  
26 processes regulating jellyfish populations over time. To this aim, stable isotopic signature  
27 analysis ( $\delta^{13}\text{C}$  and  $\delta^{15}\text{N}$ ) was used to infer the diet of both *A. coerulea* scyphistomae and  
28 medusae over one year. These results were matched with medusae gut content analysis and  
29 with the monthly abundances of local plankton groups. Lastly, the isotopic signatures of *A.*  
30 *coerulea* scyphistomae and medusae were compared with those of the oysters (*Crassostrea*  
31 *gigas*) cultivated in the lagoon to evaluate the potential interspecific trophic competition. The  
32 results revealed two seasonal shifts in the trophic niche of *A. coerulea* and substantial overlap  
33 between the diets of its benthic and pelagic stages. Conversely, trophic niche overlaps with  
34 the oysters were restricted, suggesting a limited impact of the local jellyfish bloom on  
35 shellfish production. Phytoplankton, microzooplankton, mesozooplankton, and sedimentary  
36 organic matter were all important food sources during critical periods of *A. coerulea* life-  
37 cycle. However, microzooplankton abundance was found to be key for the production of  
38 buds by the scyphistomae and, therefore it is likely to control the benthic population size and,  
39 thereby, to modulate the intensity of its annual bloom in Thau.

## 40 **Introduction**

41 Due to the impact of their conspicuous blooms on coastal ecosystems functioning and  
42 economic activities, jellyfish have received increasing scientific attention during the last  
43 decades ( Purcell 2012). In particular, the ecological drivers of jellyfish mass occurrences  
44 have been investigated, revealing a complex interaction of natural (e.g. Condon et al. 2012)  
45 and anthropogenic (e.g. Purcell 2012) causes. However, uncovering the drivers of blooms is  
46 particularly challenging for most scyphozoan blooming species because their life-cycle  
47 comprises a benthic (scyphistomae) and a pelagic (ephyrae and medusae) phase (e.g. Lucas  
48 2001). Therefore, bloom formation is a joint consequence of the production of pelagic  
49 ephyrae by the benthic scyphistomae and of their survival and growth into medusae. As a  
50 result, the ecology of both life stages controls bloom intensity.

51 Bottom-up processes within food webs often play a key role in ecological systems functioning  
52 and are amongst the most important drivers of jellyfish blooms (Boero et al. 2008). Food  
53 quality and availability are known to control the production of ephyrae by the scyphistomae  
54 (Han and Uye 2010; Ikeda et al. 2017) and to modulate the growth rate of medusae (Ishii and  
55 Båmstedt 1998). This supports the need for comprehensive studies on the trophic ecology of  
56 both life stages in the field. Yet, although information is growing on the trophic ecology of  
57 medusae (e.g. Javidpour et al. 2016; Milisenda et al. 2018), the diet of jellyfish scyphistomae  
58 is still poorly known.

59 Jellyfish from the *Aurelia* genus are present globally in coastal areas and are among the most  
60 common scyphozoans that form blooms (Mills 2001). Large accumulations of *Aurelia* spp.  
61 have been reported all around the world, including in the Mediterranean, where they occur  
62 mainly in protected waters and semi-enclosed seas (Mills 2001). Their medusae have been  
63 described as zooplanktivorous, with a dominance of mesozooplankton, especially copepods,  
64 in their diet (e.g. Ishii and Tanaka 2001; Lo and Chen 2008). However, while

65 microzooplankton and benthic food sources have been considered for long as negligible food  
66 sources for jellyfish, recent findings based on new techniques (such as stable isotope analysis)  
67 suggest the opposite (Javidpour et al. 2016). In laboratory studies, newly hatched *Artemia* sp.  
68 are usually provided as food (e.g. Han and Uye 2010, Hubot et al. 2017), but the few studies  
69 regarding the diet of *Aurelia* sp. scyphistomae in the wild suggest that they eat a mix of  
70 phytoplankton (Huang et al. 2015), microzooplankton (Kamiyama 2013) and small  
71 mesozooplankton species (e.g. copepods, cladocerans, gelatinous zooplankton; Östman 1997).  
72 Considering the critical role of scyphistomae in the formation of scyphozoans blooms, it is  
73 urgent to specify natural prey preferences in *Aurelia* species and the potential trophic  
74 competition among their benthic and pelagic stages to understand blooms formation in this  
75 genus and evaluate their ecological consequences.

76 Situated along the North-western Mediterranean coast, the Thau lagoon offered an  
77 exceptional framework for this. Indeed, this lagoon presents the rare particularity to harbour a  
78 complete resident population of *Aurelia coerulea* (Bonnet et al. 2012; Marques et al. 2015a),  
79 which allows investigating the trophic processes that regulate its population dynamics at both  
80 stages. The scyphistomae of *A. coerulea* are widespread in the lagoon, fixed mainly on  
81 biofouling organisms that grow on anthropogenic structures (predominantly on oysters and  
82 mussels; Marques et al. 2015a). They are present all year round, with a peak of coverage in  
83 the Spring (April) and lower densities in the Summer and Autumn (Marques et al. 2019).  
84 Ephyrae appear in the early winter (November – December) and give rise to adult medusae at  
85 the beginning of the Spring (April – May), generating the annual jellyfish bloom, which  
86 persists until June – July (Bonnet et al. 2012; Marques et al. 2015b). Because no clear link  
87 was found between the abundance of mesozooplankton in the lagoon and the benthic  
88 population dynamics of *A. coerulea*, it was suggested that other food sources might sustain

89 the species local production (Marques et al. 2019). Nevertheless, further confirmation is still  
90 required in this regard.

91 Coastal lagoons are usually very productive environments, where high continental inputs in  
92 nutrients and particulate organic matter sustain high and diversified primary and secondary  
93 productions (Nixon et al. 1995). This benefits the whole food web and enhances the growth of  
94 lagoon predators like juvenile fish (Escalas et al. 2015). In Thau, it also supports a massive  
95 shellfish production: ~10% of the Pacific oysters *Crassostrea gigas* produced in France come  
96 from the lagoon, with a yearly shellfish production of 15 000 tons (Mongruel et al. 2013).

97 In this context, the present work not only aimed to describe the trophic ecology of both the  
98 benthic and the pelagic life-stages of *A. coerulea* in Thau and assess its influence on critical  
99 periods of population dynamics of this jellyfish (e.g. peak of bud production, strobilation, and  
100 medusae growth), but also to evaluate whether *A. coerulea* medusae and scyphistomae  
101 compete for food with the Pacific oysters reared in the lagoon. For this, we combined  
102 medusae gut content assessments with stable isotopes analysis. This latter technique has been  
103 increasingly used to study the structure and transfer of organic matter within coastal food  
104 webs (Layman et al. 2012) and has recently allowed uncovering the diet, trophic levels, and  
105 trophic interactions of different jellyfish species (Fleming et al. 2015; Javidpour et al. 2016;  
106 Milisenda et al. 2018). Using it to explore the changes in *A. coerulea* diet during a full annual  
107 cycle should allow assessing whether its benthic and pelagic stages occupy the same trophic  
108 niche than the oysters cultivated in the lagoon. This strongly contributes to a better  
109 understanding of the impacts of *A. coerulea* blooms on the local shellfish production.

110

## 111 **Material and Methods**

112 *Study site*

113           The Thau lagoon is a semi-enclosed marine coastal lagoon of 75 km<sup>2</sup> area, connected  
114 to the Mediterranean Sea by three narrow channels (Fig. 1). It is relatively shallow, with mean  
115 and maximum depths of 4 and 10 m, respectively (except for a localized depression of 24 m).  
116 The local tidal range (< 1m) is weak, so water residence time in the lagoon is globally high  
117 (1–4 months) and strongly influenced by seasonal strong wind events (Millet and Cecchi  
118 1992). The lagoon environment parameters show strong seasonal variations, characteristic of  
119 temperate regions, with temperature and salinity at their lowest in the winter (with minimum  
120 values of 7.6 and 35.0, respectively) and at their highest in the summer (with maximum  
121 values of 25.8 °C and 39.6, respectively; Marques et al 2019). The lagoon mainly receives  
122 water from the Sète canal that connects it to the Mediterranean Sea and from several small  
123 intermittent rivers that drain its catchment area (290 km<sup>2</sup>, Plus et al. 2006). These later dry out  
124 between May and September and show occasional flash floods in the wet season (Fouilland et  
125 al. 2012). As a result, marine conditions prevail in the lagoon, the annual influence of the  
126 freshwater coming from the watershed being highly dependent on the intensity of rainfall  
127 events during the winter (Plus et al. 2006). With regards to anthropogenic influence, the  
128 lagoon is under multiple pressures due to the presence of the touristic city of Sète and many  
129 small villages and agriculture fields on its coastline. Shellfish farming is the most important  
130 economic activity on the lagoon (Mongruel et al. 2013): around 20% of its surface is occupied  
131 by farms, mainly in the northern and north-western parts (Fig. 1).

132

### 133 *Sampling*

134           For this study, the jellyfish and their potential food sources were sampled in the  
135 eastern part of the lagoon, at two close sites where the benthic and the pelagic population  
136 dynamics of *A. coerulea* had been previously described (Bonnet et al. 2012; Marques et al.  
137 2015b; Marques et al. 2019). Both sites (benthic sampling site: 43°25'31.1"N; 03°42'0.9"E

138 and pelagic sampling site: 43°23'59.1''N; 03°36'37.2''E; Fig. 1) are located on soft-bottom  
139 sediments punctuated by sparse seagrass meadows and are strongly influenced by marine  
140 water influxes due to their proximity to the Sète channel, which connects the lagoon to the  
141 Mediterranean Sea.

142 *A. coerulea* scyphistomae were collected monthly on a partially submerged boat present at  
143 the benthic sampling site (see Marques et al. 2019 for more details), over an entire calendar  
144 year (from January 2017 to January 2018). For this, mussel shells with sizeable aggregates of  
145 scyphistomae attached on their underside surface (three per sampling date) were collected  
146 directly on the surface of the boat by SCUBA diving. They were brought to the laboratory in  
147 ambient water and placed in 0.2- $\mu$ m-filtered seawater (ca. 20°C) for about 2h to ensure all  
148 scyphistomae had empty guts. Fifty individual scyphistomae were then collected under a  
149 dissecting microscope (Olympus SZ40; Olympus KL 1500 LCD), using needles and tweezers  
150 to carefully detach them, and preserved in cryotubes at -30°C.

151 The pelagic ephyrae of *A. coerulea* are usually present in the lagoon from November to April  
152 (Bonnet et al. 2012; Marques et al. 2015b). However, because stable isotope analysis requires  
153 pooling high numbers of these small organisms to be applicable, sampling for this life stage in  
154 this work was successful in January 2018 only. The ephyrae were collected near the water  
155 surface at the pelagic sampling site, by horizontal towing, using a modified WP2 plankton net  
156 (1.2 m long, 50-cm opening, and 200- $\mu$ m mesh). In the laboratory, they were picked and kept  
157 for ca. 2h in filtered seawater to allow for complete gut evacuation. Then 50 individuals were  
158 pooled per sample and preserved at -30°C.

159 *A. coerulea* medusae (i.e., pelagic individuals with bell diameter > 1 cm), were collected  
160 every two weeks at the pelagic sampling site, from March to June 2017, i.e., over the entire  
161 period of their presence in the lagoon. They were collected in surface waters using hand nets  
162 and transported to the laboratory in ambient water. Five individual medusae were then



163 randomly selected and prepared for stomach content analysis. For this, they were each  
164 partially dried on a paper towel to remove excess water, measured (bell diameter in cm),  
165 weighted (total wet weight in g), and individually preserved in 4% buffered formaldehyde.  
166 The remaining medusae were kept for ca. 2h in 0.2  $\mu\text{m}$  filtered seawater (ca. 20°C) to empty  
167 their guts. Three of them were then placed on a paper towel for about 1 minute (30 s on each  
168 side) to remove excess water, weighed, and measured. As bell tissue is the most suitable body  
169 part for stable isotope analysis in jellyfish (D'Ambra et al. 2014), gonads, oral arms, and  
170 gastric pouches were removed from each medusa. The remaining individual bell tissues were  
171 preserved separately at -30°C. In March 2017, due to the small size of the medusae (ca. 2 cm  
172 bell diameter), eight complete individuals were pooled per replicate before preservation at -  
173 30°C.

174 For this work both the plankton and the sedimentary organic matter of the lagoon were also  
175 sampled as they both constitute potential food sources for *A. coerulea*. Samples for these two  
176 components were collected at pelagic and benthic sampling sites, respectively, on the same  
177 sampling dates as *A. coerulea* medusae and scyphistomae collection. Within the plankton, the  
178 fraction larger than 200  $\mu\text{m}$ , that between 60 and 200  $\mu\text{m}$  and that between 20 and 60  $\mu\text{m}$   
179 were assumed to be composed mainly by mesozooplankton, microzooplankton, and  
180 phytoplankton, respectively. Mesozooplankton samples were collected near the surface, by  
181 horizontal towing, using a modified WP2 plankton net (length: 1.2 m; opening area: 50 cm;  
182 mesh size: 200  $\mu\text{m}$ ). Once in the laboratory, each sample was filtered through a 60  $\mu\text{m}$  mesh  
183 sieve to eliminate excess water and divided into five subsamples. Microzooplankton and  
184 phytoplankton samples were also collected by horizontal towing near the surface, but using a  
185 phytoplankton net (length: 1 m; opening area: 30 cm; mesh size: 20  $\mu\text{m}$ ). Once in the  
186 laboratory, each sample was filtered through a 200- $\mu\text{m}$  sieve. The size fraction  $> 200 \mu\text{m}$  was  
187 discarded. The remaining sample was then separated into the two size fractions,

188 corresponding to microzooplankton and phytoplankton, using a 60  $\mu\text{m}$  sieve, and then divided  
189 into 5 subsamples. For each plankton size fraction, the subsamples were collected separately  
190 on pre-combusted (500°C for 24h) Whatman GF/F filters. Two filters of each plankton  
191 component were acidified with 1% HCl and triple rinsed with distilled water to remove  
192 inorganic carbon, which can bias C stable isotope results ( Yokoyama et al. 2005). The  
193 remaining non-acidified filters were used for N stable isotope analysis, since sample  
194 acidification may affect the stable isotope signature for this element (Pinnegar and Polunin  
195 1999). All samples were preserved at  $-30^{\circ}\text{C}$  until further analysis. For sedimentary organic  
196 matter, the first 2 cm of the sediment were collected by SCUBA diving at the benthic  
197 monitoring site. Samples (2 replicates) were carefully scrutinized to eliminate any large  
198 organisms, sediment inorganic particles, or vegetal debris, before preservation at  $-30^{\circ}\text{C}$ .  
199 To investigate the trophic interactions between *A. coerulea* and the local oysters, both wild  
200 and cultivated individuals of *Crassostrea gigas* were sampled seasonally from October 2017  
201 to August 2018, including during the peak of the jellyfish bloom (which occurred in June in  
202 2018). Wild oysters (mean size:  $11.5 \pm 2.0$  cm) were collected by SCUBA diving at the  
203 benthic monitoring site, while the cultivated ones (mean size:  $11.9 \pm 1.0$  cm) were obtained  
204 from the shellfish producer *Huitres-Bouzigues.com*. Immediately after their removal from the  
205 lagoon, the oysters were transported to the laboratory in ambient water, measured and  
206 carefully dissected to collect their adductor muscle. The muscle tissues were then rinsed with  
207 distilled water and preserved separately at  $-30^{\circ}\text{C}$  until further analysis.

208

#### 209 *In situ abundance of plankton in the Thau lagoon*

210 Phytoplankton, microzooplankton and mesozooplankton samples were collected at the pelagic  
211 monitoring site, every two weeks from January to June 2017 and monthly onwards, until  
212 December 2017. For phytoplankton, 10 to 20L of surface water were collected, filtered with a

213 15- $\mu$ m-mesh net, and preserved with 2% buffered formaldehyde. For microzooplankton, a  
214 subsample of 30 ml of surface water was preserved with 2% buffered formaldehyde (to  
215 estimate ciliates' abundance) and one of 110 ml was preserved with Lugol's solution (to  
216 estimate heterotrophic flagellates' abundance). Phytoplankton and microzooplankton species  
217 were identified and counted using sedimentation chambers and an inverted microscope  
218 (Olympus IX70) following the Utermöhl method (Utermöhl 1958). Mesozooplankton samples  
219 were collected near the surface by horizontal towing using a modified WP2 plankton net (1.2  
220 m long, 50-cm opening, and 200- $\mu$ m mesh). Samples were immediately preserved in 4%  
221 buffered formaldehyde until further analysis in the laboratory. Mesozooplankton abundance  
222 was determined by counting organisms under a dissecting microscope (Olympus SZX7 –  
223 ILLT). The diversity of mesozooplankton was not assessed.

224

#### 225 *Gut content analyses*

226 To evaluate the diet of *A. coerulea* medusae, their gastric pouches, oral arms, and the  
227 preserving solution were examined under a dissecting microscope (Olympus SZX7 – ILLT).  
228 Although *A. coerulea* medusae were present in the lagoon from March, most individuals  
229 exhibited empty guts during this month. Therefore, gut content analysis was only performed  
230 on the medusae collected between April and June. For this, only complete exoskeletons were  
231 considered for prey identification. This was done to the lowest possible taxonomic level,  
232 although the level of exoskeleton digestion often precluded prey identification down to the  
233 species level. The importance of each prey in the diet was expressed by the following indices:  
234 (i) the frequency of occurrence (in %), which represents the percentage of medusae with the  
235 prey *i* in their guts among all those that had non-empty guts; (ii) the index of relative  
236 importance (in %), representing the percentage of prey *i* in relation to the total number of prey

237 items found in the non-empty guts; and (iii) the mean abundance of prey *i* in non-empty guts  
238 (in ind. medusae<sup>-1</sup>).

239

#### 240 *Stable isotope analysis*

241 All filters containing plankton (phytoplankton, microzooplankton, and mesozooplankton)  
242 were oven-dried at 60°C for 48h and the biological material was gently scraped off the filter  
243 surface. Samples for the sedimentary organic matter, the oysters, *A. coerulea* medusae,  
244 scyphistomae, and ephyrae were freeze-dried for 48h and ground to a fine powder using a  
245 mortar and pestle. The sedimentary organic matter samples were divided into two subsamples.  
246 One half was used directly for N stable isotope analysis. The remaining subsample was  
247 acidified with 1% HCl to remove carbonates before C stable isotope analysis, rinsed several  
248 times with distilled water, and oven-dried at 70°C.

249 Stable isotopic analyses for biological samples were performed using a PDZ Europa ANCA-  
250 GSL elemental analyser interfaced with a PDZ Europa 20-20 isotope ratio mass spectrometer  
251 (Sercon Ltd., Cheshire, UK). Measurements of  $\delta^{13}\text{C}$  and  $\delta^{15}\text{N}$  signatures were performed each  
252 on 1.5 to 4 mg of dry samples, with exception of the medusae, for which ca. 10 mg of dry  
253 sample was required for successful analysis, after salt content correction, based on dry weight  
254 and ash-free dry weight relationships (Lucas et al. 1994; Pitt et al. 2009). Sedimentary organic  
255 matter samples (of ca. 55 mg each) were analysed using an Elementar Vario EL Cube or  
256 Micro Cube elemental analyser (Elementar Analysensysteme GmbH, Hanau, Germany)  
257 interfaced to a PDZ Europa 20-20 isotope ratio mass spectrometer (Sercon Ltd., Cheshire,  
258 UK). Calibration was performed against NIST Standard Reference Materials (IAEA-600,  
259 USGS-40, USGS-41, USGS-42, USGS-43, USGS-61, USGS-64, and USGS-65). Isotope  
260 ratios of all samples were expressed as parts per thousand (‰) differences from the internal

261 reference standards (glutamic acid, alfalfa flour, nylon 6, bovine liver, and enriched alanine)  
262 using the following equation:

$$263 \quad \delta X = \left[ \left( \frac{R_{sample}}{R_{standard}} \right) - 1 \right] \times 1000$$

264 where  $X$  is the  $^{13}\text{C}$  or  $^{15}\text{N}$  and  $R$  is the corresponding ratio,  $^{13}\text{C}/^{12}\text{C}$  or  $^{15}\text{N}/^{14}\text{N}$ .

265 As the lipid content of organisms affects their  $\delta^{13}\text{C}$  signatures,  $\delta^{13}\text{C}$  correction is required

266 when C:N is higher than 3.5 (Post et al. 2007). Therefore, the  $\delta^{13}\text{C}$  values obtained for *A.*

267 *coerulea* scyphistomae and medusae (mean C:N  $3.7 \pm 0.1$  and  $3.9 \pm 0.6$ , respectively) and for

268 the mesozooplankton (mean C:N of  $6.9 \pm 3.0$ ) were corrected ( $\delta^{13}\text{C}_{corr}$ ) according to the

269 equations proposed by D'Ambra et al. (2014) for jellyfish:

$$270 \quad \delta^{13}\text{C}_{corr} = \delta^{13}\text{C}_{initial} - 9.43 + 2.69 \times C:N$$

271 and by Syväranta and Rautio (2010) for zooplankton:

$$272 \quad \delta^{13}\text{C}_{corr} = \delta^{13}\text{C}_{initial} + 7.95 \times \left( \frac{C:N - 3.8}{C:N} \right)$$

273

274

### 275 *Relationship between benthic population dynamics and plankton abundance*

276 Data on *A. coerulea* benthic population dynamics were obtained from Marques et al. (2019).

277 Generalized linear models (using linear and logistic regressions, without interactions) were

278 employed to assess the respective contributions of the absolute abundances of the non-

279 averaged phytoplankton, the microzooplankton and the mesozooplankton (after logarithmic

280 transformation  $\ln(x+1)$ ) to temporal trends in the scyphistomae density (% coverage) and in

281 the proportion of the scyphistomae producing buds. The models were validated by

282 examination of residuals versus fitted values plots (Zuur et al. 2009).

283

### 284 *Determination of Isotopic Niche Periods*

285 To reveal potential shifts in the trophic niches of *A. coerulea* scyphistomae and medusae  
286 during the year and identify the periods when they present unchanging isotopic signatures  
287 (hereafter "Isotopic Niche Periods"), a cluster analysis was performed on the monthly mean  
288 isotopic values of both life stages (Jain 2010). For this, partitioning algorithms, based on the  
289 k-means clustering method, were applied using the package "factoextra" (Kassambara and  
290 Mundt 2017). The k-means approach subdivides the data into a set of k groups so that the sum  
291 of squares from the data points to the center of each group is minimized (Kassambara and  
292 Mundt 2017). This clustering approach allowed to identify the successive isotopic niche  
293 periods for both life stages, providing the basis for identifying their successive sources of  
294 organic matter during the year.

295

#### 296 *Assessment of potential intra- and interspecific trophic competition*

297 Our sampling design allowed for reliable estimation of the potential intraspecific trophic  
298 competition between *A. coerulea* scyphistomae and medusae within each isotopic niche  
299 period. However, because oyster and jellyfish samples were collected in different years  
300 (except for one isotopic niche period), the trophic competition between the two species was  
301 only investigated globally, assuming that interannual variability in the trophic niche in the two  
302 species is negligible. In both cases, the Bayesian framework proposed by Jackson et al. (2011)  
303 for evaluating trophic competition was used. For this, Bayesian multivariate normal  
304 distributions were first fitted to the isotopic signatures of all organisms. Then, the overlap  
305 between their trophic niches was calculated based on maximum likelihood fitted ellipses,  
306 using the function "maxLikOverlap" from the R package "SIBER" (Jackson et al. 2011).

307

#### 308 *Determination of jellyfish diet using Stable isotope analysis*

309 Differences in isotopic signatures ( $\delta^{13}\text{C}$  and  $\delta^{15}\text{N}$ ) among the main local potential food  
310 sources (phytoplankton, microzooplankton, mesozooplankton, and sedimentary organic  
311 matter) were tested by a PERMANOVA (Anderson 2017) on the log10 transformed Bray-  
312 Curtis distance matrix ( $-\delta^{13}\text{C}$  and  $\delta^{15}\text{N}$ ), made using the package “vegan” (Oksanen et al.  
313 2019), followed by pairwise comparisons made using the “pairwiseAdonis” package in R  
314 (Martinez Arbizu 2019). Sources with no significant differences were grouped for subsequent  
315 analyses.

316 Diet compositions for *A. coerulea* scyphistomae and medusae within each isotopic niche  
317 period were assessed using Bayesian mixing models developed specifically for stable isotope  
318 analysis (“MixSIAR” package, Stock and Semmens 2016). By generating the probability  
319 distributions of all potential mixing solutions with the associated confidence intervals (based  
320 on 300 000 chain length), this approach allows identifying the most likely contribution for  
321 each food source. MixSIAR further provides a graphical user interface that allows  
322 investigation of the contributions of multiple food sources to the diet of target predators,  
323 considering not only the isotopic signatures ( $\delta^{13}\text{C}$  and  $\delta^{15}\text{N}$ ) of the sources and the predators  
324 but also the uncertainties and variability around these estimates. Finally, the method allows us  
325 to use different isotopic fractionation factors at each trophic level. As previously performed in  
326 other studies on jellyfish diet (e.g. Morais et al. 2017), the fractionation values applied here  
327 for both *A. coerulea* life stages were those proposed by Vander Zanden and Rasmussen  
328 (2001): for  $\delta^{13}\text{C}$  we used  $0.47 \pm 1.23$  ‰ in all cases, while for  $\delta^{15}\text{N}$  we used  $2.52 \pm 2.5$  ‰ and  
329  $3.23 \pm 0.41$  ‰ according to the type of food consumed (plant vs. animal, respectively). Like  
330 Fleming et al. (2015) and Milisenda et al. (2018), we did not use the fractionation values  
331 reported by D’Ambra et al. (2014), since they are very distinct from those mostly used in the  
332 literature (Vander Zanden and Rasmussen 2001; Post 2002) and they still require further  
333 laboratory corroboration (D’Ambra et al. 2014).

334 The basal tissue turnover rate for *Aurelia* sp. is of ca. 1 ‰ day<sup>-1</sup> for  $\delta^{13}\text{C}$  and 2‰ day<sup>-1</sup> for  
335  $\delta^{15}\text{N}$ , and it takes 18 to 20 days for the tissues of this jellyfish to reach the stable isotopic  
336 equilibrium with the food ingested (D'Ambra et al. 2014). To account for such turnover rates,  
337 MixSIAR models were run by isotopic niche period, but jellyfish signatures at a given  
338 sampling date were matched with those recorded one month earlier for all potential food  
339 sources.

340

## 341 **Results**

### 342 *Medusae gut contents*

343 Among the 25 medusae collected for gut content analysis from April to June 2017, 21 had  
344 food in their guts. The bell diameter of these individuals did not vary significantly over time  
345 (ANOVA,  $F_2 = 1.4$ ,  $p\text{-value} = 0.2$ ), remaining at ca. 8.5 cm. Overall, gut content composition  
346 predominantly consisted of mesozooplankton (>88%). Microzooplankton (mainly tintinnids)  
347 and phytoplankton (mainly diatoms and dinoflagellates) represented only 8 and 4% of the  
348 total prey identified, respectively, and they were only found in the guts in April and May (Fig.  
349 2, Table 1, Supplementary Table 1). In April, phytoplankton and microzooplankton occurred  
350 in 20 and 60% of the guts analysed, but their relative importance and abundances were still  
351 low (< 7.5% and < 2.2 ind.medusa<sup>-1</sup>, respectively, Table 1). In May, frequency of occurrence  
352 increased for phytoplankton (33%) and slightly decreased for microzooplankton (56%) and  
353 showed a growing trend of their relative importance for both groups (5.6 and 12.5%,  
354 respectively, Fig. 2). Indeed, in May, microzooplankton relative importance was higher than  
355 some mesozooplankton organisms, like the “other crustaceans” group, which includes  
356 cladocerans and ostracods (10.0%; Table 1, Supplementary Table 1). Masses of unidentified  
357 organic matter were also recurrently observed over the entire study period.



358 Twenty-four different taxa of mesozooplankton were identified in the guts of the medusae,  
359 but, among them, copepods and nauplii (from cirripeds and copepods) dominated. They  
360 occurred in 40 to 88.9% of the guts analysed and represented up to 46.3% of the prey  
361 identified (in June, Table 1). The maximum average abundance of mesozooplankton  
362 organisms in the guts ( $26.2 \pm 35.4$  ind.medusae<sup>-1</sup>) was recorded in April when non-crustacean  
363 taxa (mainly gastropod veliger), and copepods represented more than 80% of the prey  
364 identified in medusae gut contents (Table 1). Nauplii (index of relative importance = 31.3%)  
365 were the most important mesozooplanktonic prey in the guts in May, while in June, copepods  
366 dominated (index of relative importance = 46.3%, Table1).

367

#### 368 *Prey availability and relationship with benthic population dynamics*

369 Prey abundances in *A. coerulea* medusae gut contents did not reflect their availability in the  
370 water column. The abundances of phytoplankton, microzooplankton, and mesozooplankton in  
371 the lagoon all showed high intra-annual variability (Fig. 3), with respective peaks in January  
372 ( $25\,138 \pm 34\,047$  cell.L<sup>-1</sup>) and May ( $35\,794 \pm 18\,374$  and cell.L<sup>-1</sup>), in February, April, and  
373 September ( $> 6\,200$  cell.L<sup>-1</sup>) and in June ( $90\,895 \pm 107\,072$  ind.m<sup>-3</sup>). Thus, when *A. coerulea*  
374 medusae were present in the water column, the planktonic community was mainly dominated  
375 by phytoplankton in April and May, and by mesozooplankton in March and June, while the  
376 microzooplankton showed consistently lower abundances despite a small peak in April. In  
377 terms of species composition, the most abundant phytoplanktonic and microzooplanktonic  
378 taxa in the water column during the study period were *Chaetoceros* sp. and *Strombidium* sp.,  
379 respectively (Supplementary Table 2). Mesozooplankton diversity was not assessed, but  
380 *Acartia* sp. are recurrently the most abundant taxa in Thau (Boyer et al. 2013).  
381 Annual variations in scyphistomae coverage, which peaked in April ( $11.6 \pm 3.7$  %, Marques  
382 et al. 2019), were positively correlated with the non-averaged abundance of phytoplankton

383 (Generalized linear models, t-value = 2.97, p-value = 0.01, Table 2, Fig. 4). In turn,  
384 fluctuations in the mean percentage of scyphistomae producing buds, which varied between  
385  $0.4 \pm 0.7$  % in November and  $25.2 \pm 7.3$  % in September (Marques et al. 2019, Fig. 4), were  
386 positively correlated with variations in non-averaged microzooplankton abundance  
387 (Generalized linear models, t-value = 10.19, p-value < 0.01, Table 2).

388

### 389 *Temporal variation of A. coerulea isotopic signatures*

390  $\delta^{13}\text{C}$  and  $\delta^{15}\text{N}$  signatures showed significant temporal variation for both the scyphistomae and  
391 medusae (one-way PERMANOVA, Pseudo- $F_{11} = 22.7$ , p-value < 0.01 and Pseudo- $F_3 = 38.6$ ,  
392 p-value = 0.001, respectively), but differences between life stages were never significant  
393 during the period of medusae presence, from March to June (one-way PERMANOVA,  
394 Pseudo- $F_1 = 1$ , p-value = 0.4). The mean bell diameter of the medusae used for stable isotope  
395 analysis, showed a sharp increase between March ( $1.0 \pm 0.3$  cm) and June ( $8.9 \pm 1.1$  cm), with  
396 an estimated overall growth of  $0.8 \text{ mm}\cdot\text{day}^{-1}$ . Over this period, medusae  $\delta^{13}\text{C}$  signatures  
397 increased progressively from  $-23.4 \pm 0.1\text{‰}$  to  $-19.4 \pm 0.5\text{‰}$ , while their  $\delta^{15}\text{N}$  signatures  
398 remained stable for the first three months (at ca.  $8.1\text{‰}$ ), and increased (to a maximum at  $8.9 \pm$   
399  $0.3\text{‰}$ ) only in June (Fig. 5). For the scyphistomae, minimum  $\delta^{13}\text{C}$  values were registered at  
400 the beginning of the study period (in January 2017, mean:  $-23.4 \pm 0.1\text{‰}$ ). The  $\delta^{13}\text{C}$  signatures  
401 then increased to reach maximum values in June, July, and August ( $> -19.4\text{‰}$ ) before  
402 decreasing again until January 2018 ( $-22.3 \pm 0.4\text{‰}$ ). The  $\delta^{15}\text{N}$  signatures of scyphistomae  
403 showed a similar temporal trend, with low values at the beginning and the end of the study  
404 period ( $8.3 \pm 0.1\text{‰}$  and  $8.0 \pm 0.4\text{‰}$  in January 2017 and 2018, respectively), and maximum  
405 values in July and August ( $>9\text{‰}$ ). The minimum values of  $\delta^{15}\text{N}$  signatures, though, were  
406 observed in February 2017 ( $7.1 \pm 0.5\text{‰}$ ). The average  $\delta^{13}\text{C}$  and  $\delta^{15}\text{N}$  signatures of the ephyrae  
407 collected in January 2018 (bell diameter of  $0.21 \pm 0.1$  cm) were of  $-22.8 \pm 0.1\text{‰}$  and  $8.5 \pm$

408 0.3‰, respectively. They did not differ significantly from those of the scyphistomae collected  
409 at the same sampling time (T-test,  $t = -1.9$ ,  $df = 2.3$  p-value = 0.2 and  $t = 1.2$ ,  $df = 2.6$ , p-value  
410 = 0.3, for  $\delta^{13}\text{C}$  and  $\delta^{15}\text{N}$  respectively).

411 The clustering analysis revealed three distinct groups of isotopic signatures among the  
412 monthly values obtained for all life stages of *A. coerulea* (Fig. 6) allowing to identify three  
413 isotopic niche periods during the year.: Period 1 gathered the  $\delta^{13}\text{C}$  and  $\delta^{15}\text{N}$  signatures of all  
414 life stages from December to April, irrespective of the year (2017 or 2018). Period 2 reflected  
415 the signatures of both the medusae and the scyphistomae from June to August. Period 3  
416 corresponded to the signatures of the scyphistomae from September to November, together  
417 with the signatures of the medusae and the scyphistomae in May. However, May showed a  
418 particular sharp shift in  $\delta^{13}\text{C}$  and  $\delta^{15}\text{N}$  reflecting the rapid transition from the isotopic  
419 signature of period 1 to that of period 2 and, therefore, it was not included in any isotopic  
420 niche period.

421

#### 422 *Monthly variability of organic matter sources signatures*

423  $\delta^{13}\text{C}$  and  $\delta^{15}\text{N}$  signatures varied significantly according to the organic matter source and the  
424 month (significant interaction, PERMANOVA,  $Pseudo-F_{17} = 23.1$ , p-value < 0.01; Fig. 7).  
425 For carbon signatures, minimum  $\delta^{13}\text{C}$  values for phytoplankton, microzooplankton and  
426 mesozooplankton (of  $-24.7 \pm 0.3$ ,  $-23.3 \pm 0.1$  and  $-23.7 \pm 0.0$  ‰, respectively) were all  
427 observed in March. A sharp increase in  $\delta^{13}\text{C}$  was observed in the following months, with  
428 maximums in May for mesozooplankton ( $-18.8 \pm 0.2$  ‰) and in November for phytoplankton  
429 ( $-19.0 \pm 0.0$  ‰) and microzooplankton ( $19.9 \pm 0.1$  ‰). Concerning nitrogen signatures,  
430 mesozooplankton was the organic matter source with the highest  $\delta^{15}\text{N}$  values, ranging from  
431  $7.3 \pm 0.3$  (in May) to  $8.4 \pm 0.0$ ‰ (in March). Minimum  $\delta^{15}\text{N}$  values were also observed in  
432 May for the phytoplankton and the microzooplankton (at  $5.8 \pm 0.5$  ‰ and  $6.0 \pm 0.3$  ‰,

433 respectively) but, for these two organic matter sources, maximum values were observed in  
434 July (at  $6.7 \pm 0.3$  ‰ and  $7.4 \pm 0.2$  ‰, respectively). Moreover, another peak in  $\delta^{15}\text{N}$  (at  $6.7 \pm$   
435  $0.0$  ‰) was observed in February for the phytoplankton. For the sedimentary organic matter,  
436 both the  $\delta^{13}\text{C}$  and  $\delta^{15}\text{N}$  signatures decreased from March ( $-18.9$ ‰ and  $5.8$ ‰, respectively) to  
437 April ( $-20.7$ ‰ and  $5.5$ ‰, respectively), remaining constant afterwards.

438

#### 439 *Contribution of organic matter sources to A. coerulea isotopic signatures*

440 Since the  $\delta^{13}\text{C}$  and  $\delta^{15}\text{N}$  signatures of the phytoplankton and the microzooplankton were not  
441 significantly different (PERMANOVA post-hoc test, Pseudo- $F_1 = 5.7$ , adjusted p-value =  
442  $0.17$ ) these two organic matter sources were pooled as Small Plankton group in the mixing  
443 models used to assess the diet of *A. coerulea*. The remaining sources were included  
444 individually in the models (Table 3). The contribution of each source was found to vary  
445 according to the isotopic niche periods and the life stage of *A. coerulea* considered (Fig. 8).  
446 For the scyphistomae, the model suggested a dietary shift from small plankton consumption in  
447 period 1 (93.3%) to a diet based on a mix of benthic (36.6% of sedimentary organic matter)  
448 and pelagic (39.3% of mesozooplankton and 24.4% of small plankton) sources in period 2.  
449 The same occurred in period 3, although the small plankton was the main food source  
450 (69.2%), and sedimentary organic matter contribution decreased (27.0%). For the medusae,  
451 small plankton was the only food source (100%) in period 1, but the diet changed in period 2,  
452 including mainly sedimentary organic matter (64.3%) and mesozooplankton (32.3%). As the  
453 isotopic signatures of the ephyrae collected in January 2018 were very similar to those of the  
454 scyphistomae in the same period, their diet probably mainly consist of small plankton  
455 organisms.

456

#### 457 *Intra- and interspecific competitions for the food resources*

458 Intraspecific isotopic niche overlap was substantial during the whole period of co-occurrence  
459 of the benthic and pelagic stages of *A. coerulea* in the lagoon (March to June; Fig. 9). Indeed,  
460 although the percentage of niche overlap was higher in period 1 (41.5%) than in period 2  
461 (only 9.9%), the isotopic niche of the medusae entirely overlaid that of the scyphistomae in  
462 period 2. Similarly, although only three ephyrae samples were analysed in this study (all from  
463 January 2018), their isotopic signatures were close to those observed for the scyphistomae in  
464 period 1, suggesting high (although not quantifiable) trophic niche overlap among these two  
465 life stages.

466 In Thau, interspecific trophic competition between *A. coerulea* and bivalves was observed,  
467 although limited. The  $\delta^{13}\text{C}$  and  $\delta^{15}\text{N}$  signatures of the oysters from the lagoon varied from –  
468 25.6 to –18.5 ‰ and from 8.4 to 9.4‰, respectively (Fig. 10). Significant differences in  
469 isotopic signatures were observed between cultivated and wild individuals (PERMANOVA,  
470 Pseudo- $F_{11} = 12.4$ ,  $p\text{-value} < 0.01$ ; Fig. 10), with the former showing significantly higher  $\delta^{13}\text{C}$   
471 ( $-19.7 \pm 0.9$  ‰) and lower  $\delta^{15}\text{N}$  ( $8.6 \pm 0.3$  ‰) signatures on average than the later ( $-20.1 \pm$   
472  $0.4$  ‰ and  $9.2 \pm 0.3$  ‰, respectively). Interspecific isotopic niche overlaps were limited  
473 (<30%) and lower than that between cultivated and wild oysters (35.4%). Interspecific  
474 isotopic niche overlap was more important between cultivated oysters and *A. coerulea* medusa  
475 stage (29.1%). However, if we assume that the seasonal shifts in isotopic signatures are  
476 consistent among years for both the jellyfish and the oysters, the trophic competition for food  
477 should only occur at a limited period of the year and only with the medusae stage. Indeed,  
478 only the signatures recorded in period 2 were responsible for the interspecific niche overlap  
479 observed among *A. coerulea* medusae and cultivated (21.8%) or wild (21.1%) oysters.

480

## 481 **Discussion**

482 To our knowledge, this is the first study to investigate the trophic ecology of both the benthic  
483 and the pelagic stages of a jellyfish species (*A. coerulea*) in association with its in situ  
484 population dynamics and the plankton availability. The results obtained offer the  
485 unprecedented opportunity to identify the bottom-up processes regulating *A. coerulea*  
486 populations, contributing to our understanding of the formation of its blooms.

487

#### 488 *Trophic ecology of the pelagic stages of A. coerulea*

489 Ephyrae were only collected once during the study period and their isotopic signature was  
490 similar to that of scyphistomae at the same time, indicating major importance of the small  
491 planktonic organic matter (i.e. phytoplankton and microzooplankton) in their diet. This result  
492 will have to be confirmed because, in Thau, *A. coerulea* ephyrae are mainly released in  
493 November, but strobilation continues until April (Marques et al. 2019). Therefore, we cannot  
494 exclude that the ephyrae caught in January 2018 had been released just a few days or weeks  
495 before their collection and therefore still had the isotopic signature of the scyphistomae that  
496 produced them. Moreover, because of their very low growth rate during the winter ( $< 0.1$   
497  $\text{mm}\cdot\text{day}^{-1}$ , Marques et al. 2015b), the ephyrae caught in January might not have yet  
498 incorporated the signature of the prey ingested after their release (Frazer et al. 1997).  
499 Nevertheless, phytoplankton, microzooplankton (such as rotifers) and suspended particulate  
500 organic matter have all been previously identified as important food sources for ephyrae  
501 (Båmstedt et al. 2001; Zheng et al. 2015) so our findings are in agreement with the literature.  
502 The results from medusae gut contents analysis support previous reports describing *A.*  
503 *coerulea* medusae as mesozooplanktivorous, feeding mainly on copepods and nauplii (mainly  
504 of cirripeds). Indeed, *Aurelia* spp. medusae have been suggested to prey mainly on  
505 mesozooplankton and to have higher clearance rates and selective preferences for crustacean  
506 prey such as copepods, cirriped nauplii, and cladocerans (Hansson 2006; Lo and Chen 2008).

507 Phytoplankton and microzooplankton also contributed to the diet of *A. coerulea* medusae in  
508 Thau, but only during their first two months of growth and with low relative importance.  
509 Indeed, *Aurelia* spp. diet often echoes prey local abundances in their environment (e.g. Ishii  
510 and Tanaka 2001), which might explain these results, since the abundance of  
511 microzooplankton and phytoplankton in the lagoon were higher in April and May. Yet,  
512 variations of prey availability in Thau were not entirely reflected in *A. coerulea* medusae diet,  
513 since mesozooplankton represented consistently more than 80% of the prey identified in their  
514 guts, despite its lower in situ abundance in this period. Although gut content analyses  
515 provided important qualitative information on the diet of jellyfish medusae, conclusions  
516 regarding the importance of each prey type for their growth, at longer time scales, should be  
517 drawn with caution, due to the bias associated with this technique. The digestion time of  
518 mesozooplankton in the medusae guts might vary between 1 and 5h, depending on medusa  
519 size, temperature, and prey type (Ishii and Tanaka 2001; Martinussen and Båmstedt 2001),  
520 with smaller prey being digested faster (Martinussen and Båmstedt 2001). Therefore, gut  
521 content analysis often leads to an overestimation of the importance of hard and big prey in the  
522 diet, such as crustaceans. This might have contributed to a general overlook of the potential  
523 relevance of the lower trophic levels to the diet of jellyfish (Javidpour et al. 2016). Indeed, in  
524 Thau, the diet composition of *A. coerulea* medusae differed between gut content and stable  
525 isotope analyses. The later approach underlined not only the importance of the phytoplankton  
526 and microzooplankton (pooled as small plankton) for the diet of *A. coerulea* medusae in Thau  
527 but also that of the sedimentary organic matter.

528 The diet of the *A. coerulea* medusae varied over time. In general, the  $\delta^{13}\text{C}$  (–23.4 to –19.4‰)  
529 and  $\delta^{15}\text{N}$  (8.1 to 8.9‰) values found for the *A. coerulea* medusae stage were in the range of  
530 the values published by Fleming et al. (2015) (–20.3 to –18.1 for  $\delta^{13}\text{C}$  and 8.5 to 11.8 for  
531  $\delta^{15}\text{N}$ ) and D’Ambra et al. (2013) (  $-20.5 \pm 0.3\text{‰}$  and  $7.2 \pm 0.4\text{‰}$  on average for  $\delta^{13}\text{C}$  and

532  $\delta^{15}\text{N}$ , respectively). However, intra-annual fluctuations in medusae isotopic signatures  
533 revealed a significant shift in May, with an increase of ca. 3.5 and 1‰ for  $\delta^{13}\text{C}$  and  $\delta^{15}\text{N}$ ,  
534 respectively. This separates two distinct periods of stable isotopic signatures: period 1, during  
535 medusae growth from March to April, and period 2, in June, when they reproduce before the  
536 collapse of the bloom. This variation in the isotopic signature might indicate a rapid ontogenic  
537 shift in the diet of the medusae, reflecting the change from small plankton to  
538 mesozooplankton and sedimentary organic matter sources. A similar shift in the trophic niche  
539 was also shown for *Aurelia aurita* in Northern Ireland, where medusae fed on higher trophic  
540 levels by the end of their growing period (Fleming et al. 2015). Temporal variations in  
541 isotopic signatures of predators might also reflect analogous changes in the isotopic signatures  
542 at the base of the food webs (Post 2002). In this study, the values of the assessed organic  
543 matter sources agree with those previously reported in Thau (Pernet et al. 2012) and other  
544 north-western Mediterranean coastal lagoons (Dierking et al. 2012; Escalas et al. 2015) but  
545 revealed significant fluctuations over time. In Thau,  $^{13}\text{C}$ -depleted coastal inputs are dependent  
546 on the rainfall, which was high in March and low in April ([http://www.meteofrance.fr/climat-  
547 passe-et-futur/bilans-climatiques/bilan-2017](http://www.meteofrance.fr/climat-passe-et-futur/bilans-climatiques/bilan-2017). Accessed 27 Jul 2019), likely contributing to the  
548 variation in the  $\delta^{13}\text{C}$  isotopic signatures of the lower trophic levels and then reflected in those  
549 of *A. coerulea* medusae. However, similar trends were not observed for  $\delta^{15}\text{N}$  isotopic  
550 signatures, which showed a decreasing trend for most organic matter sources in May,  
551 contrasting with an increasing trend for medusae in June. This underlines that the observed  
552 isotopic niche shift for *A. coerulea* medusae was not only a reflection of temporal fluctuations  
553 in the signatures of their prey but likely induced by a significant change in their diet. Finally,  
554 our results highlight the importance of sedimentary organic matter (64.3%) in the diet of *A.*  
555 *coerulea* medusae, as previously observed for *A. aurita* in the Kiel Fjord (Javidpour et al.  
556 2016). Like most shallow marine ecosystems, the Thau lagoon is recurrently subjected to



557 sediment resuspension, triggered by river floods and strong wind activity (Fouilland et al.  
558 2012). With this regard, the unidentified masses of organic matter found in the guts of the  
559 medusae were probably aggregates of re-suspended sedimentary organic matter.

560

561 *Trophic ecology of the benthic stage of A. coerulea*

562 The temporal variability of the  $\delta^{13}\text{C}$  and  $\delta^{15}\text{N}$  signatures of *A. coerulea* scyphistomae  
563 suggested two significant intra-annual shifts in their diet and identified three different isotopic  
564 niche periods. The diet of scyphistomae was mostly based on small plankton during period 1,  
565 included all available food sources during period 2 and changed to a mix of pelagic (i.e., small  
566 plankton) and sedimentary organic matter during period 3. These seasonal variations agree  
567 with those of the availability of planktonic food sources in the lagoon, following the high  
568 abundances of phytoplankton and microzooplankton in periods 1 and 3 and that of  
569 mesozooplankton in period 2 (i.e., in June). Our results agree with the few existing reports on  
570 the diet of jellyfish scyphistomae, which suggested that they feed on small mesozooplankton  
571 species (e.g. copepods, cladocerans, and cirripeds nauplii; Östman 1997; Ikeda et al. 2017), as  
572 well as on microzooplankton and phytoplankton (dinoflagellates, ciliates, rotifers, and  
573 diatoms; Kamiyama 2013; Wang et al. 2015; Huang et al. 2015). However, as for medusae,  
574 the temporal variation in scyphistomae isotopic signatures might also reflect the origin of the  
575 carbon and nitrogen inputs in the lagoon (Post 2002). Indeed, fluctuations in  $\delta^{13}\text{C}$  and  $\delta^{15}\text{N}$   
576 values might reflect the stronger contribution of terrestrial inputs to the basis of the food web,  
577 after rainy events in period 1 (Vizzini et al. 2005; Pernet et al. 2012a) and the exceptionally  
578 low terrestrial inputs from June onwards (periods 2 and 3), due to a very dry summer and  
579 autumn in 2017 (> 80% loss of rainfall when compared with the mean between 1981 – 2010  
580 in October, <http://www.meteofrance.fr/climat-passe-et-futur/bilans-climatiques/bilan-2017>.  
581 Accessed 27 Jul 2019). Furthermore, it might also be affected by the higher influence of

582 wastewater effluent in the lagoon during dry periods (Perrin and Tournoud 2009), which is  
583 suggested to induce an enrichment of  $\delta^{15}\text{N}$  signatures, as in other coastal lagoons (Vizzini et  
584 al. 2005; Dierking et al. 2012; Escalas et al. 2015). Yet, the skewed temporal pattern of the  
585 scyphistomae isotopic signatures when compared with their sources further confirm a  
586 seasonal variation in their diet.

587 The increase in mesozooplankton consumption during period 2, when the abundance of this  
588 prey is maximal, is not surprising. Higher abundances of this type of prey (especially of newly  
589 hatched *Artemia* sp.) is recognized to induce better performances of scyphistomae (i.e.,  
590 growth, asexual reproduction, and strobilation) in laboratory experiments (e.g. Ikeda et al.  
591 2017; Hubot et al. 2017). However, our results further highlight the prominent role of the  
592 lower trophic levels in the feeding and benthic population dynamics of the species in Thau.

593 Although we were not able to precisely quantify the relative importance of phytoplankton and  
594 microzooplankton in the diet of *A. coerulea* scyphistomae, they both appear to be important.

595 Phytoplankton cells are seemingly insufficient to support scyphistomae basic metabolic rates  
596 at high temperatures (20°C) and for long periods (Wang et al. 2015; Huang et al. 2015), but  
597 they provide a suitable alternative source of energy for their survival and asexual reproduction  
598 at low temperatures (Huang et al. 2015; Wang et al. 2015). Therefore, peaks in phytoplankton  
599 abundances during period 1 probably support *A. coerulea* scyphistomae survival over the  
600 winter and early spring. Similarly, the significant positive correlation between the abundance  
601 of microzooplankton and the percentage of scyphistomae producing buds suggests that this  
602 type of prey promotes the buds production, ultimately driving the benthic population density.

603 Indeed, buds production by scyphistomae of *Aurelia aurita* has been previously shown to  
604 increase when reared on a ciliate-based diet rather than on the larger *Artemia* prey (Kamiyama  
605 2013). Interestingly, although more buds were produced in April in the lagoon (due to high  
606 scyphistomae density) the peak of the percentage of scyphistomae producing buds, as well as

607 the maximum number of buds per scyphistoma, were registered in September (Marques et al.  
608 2019), co-occurring with high abundances of microzooplankton in the lagoon.  
609 Lastly, as for medusae, our results highlight the importance of the sedimentary organic matter  
610 in the diet of *A. coerulea* scyphistomae in Thau. This does not come as a major surprise  
611 because re-suspended sediments were often observed on the scyphistomae samples collected  
612 *in situ*. Sedimentary organic matter is usually composed by a mixture of microphytobenthos,  
613 heterotrophic microorganisms (bacteria, ciliates, protozoans, nematodes) and detritus,  
614 classically associated and re-suspended with sediment (Dubois et al. 2007), which might  
615 provide a suitable source of food for jellyfish benthic stages (Östman 1997).

616

#### 617 *Intra- and interspecific competition*

618 The benthic scyphistomae and the pelagic medusae of *A. coerulea*, although inhabiting  
619 different habitats, appeared to share, at least partially, the same organic matter sources in the  
620 lagoon. During period 1, their high isotopic niche overlap, and the results of the mixing  
621 models, indicate that both stages feed on phytoplankton and/or microzooplankton. In period 2,  
622 despite a lower isotopic niche overlap, the trophic niche of the medusae entirely covers that of  
623 the scyphistomae. This suggests that during large medusae blooms and under food limitation  
624 conditions, intraspecific competition for food might occur in the lagoon, with possible  
625 detrimental impacts on the scyphistomae population.

626 One of the main concerns regarding the presence of *A. coerulea* in Thau is the potential  
627 competition for food with the oysters produced in the lagoon, in particular during the medusae  
628 blooms and due to the overspread distribution of scyphistomae (Marques et al. 2015a).

629 However, our results suggest only a limited trophic niche overlap. Although oysters and *A.*  
630 *coerulea* stages were not collected in the same year (except in period 3) we assumed that the  
631 isotopic signature of the oysters mostly varies intra-annually (Pernet et al. 2012). If this is

632 true, our results indicate that interspecific competition for food only potentially occurs  
633 between *A. coerulea* medusae and oysters (cultivated and wild) in period 2. During this  
634 period, sedimentary organic matter was an important source in the diet of *A. coerulea*  
635 medusae and also reported as part of the diet of oysters (Dubois and Colombo 2014). This  
636 might explain the isotopic niche overlap, although restricted, between these two organisms at  
637 this period. The limited interspecific trophic competition between the *A. coerulea* and the  
638 oysters might result from their different filtration and particle retention mechanisms, as  
639 previously suggested for other suspension-feeding species co-occurring with oysters (Dubois  
640 and Colombo 2014). Indeed, *A. coerulea* medusae are cruising predators, capturing their prey  
641 using locally generated flow currents (Dabiri et al. 2005) and the scyphistomae use a passive  
642 ambush strategy (Huang et al. 2015), contrasting with the true filter-feeding strategy of the  
643 oysters (Dubois et al. 2007; Dubois and Colombo 2014). The different mechanisms to capture  
644 prey, likely promoted the selection and ingestion of different organic matter sources, reducing  
645 the trophic competition for the same type of prey. Phytoplankton (especially diatoms) is the  
646 main source of food for oysters (Dupuy et al. 2000; Pernet et al. 2012). In situ feeding  
647 experiments showed that the consumption of *Aurelia* sp. medusae on micro- and  
648 mesozooplankton organisms released the predation pressure from these secondary producers  
649 on the lower trophic levels, boosting phytoplankton biomass and bacterial production (Turk et  
650 al. 2008). Therefore, it is possible that the blooms of *A. coerulea* medusae might even be  
651 advantageous for the production of oysters in the lagoon, via a top-down cascade effect on the  
652 microbial community.

653

#### 654 *Bottom-up control of the A. coerulea population dynamics*

655 In the Thau lagoon, the winter and early spring are critical periods for the formation of  
656 the *A. coerulea* bloom (Marques et al. 2019). The production of ephyrae occurs between

657 November and April, with two main peaks: in November (during period 3) due to a high  
658 percentage of the scyphistomae strobilating (despite their low densities), and in February –  
659 March (during period 1), when this percentage is low but the density of scyphistomae is high  
660 (Marques et al. 2019). As they grow to become medusae, the magnitude of the bloom is thus,  
661 tightly dependent on the accumulated production of ephyrae, their survival, and growth rate.  
662 In period 1, phytoplankton and microzooplankton are the main sources of food for both the  
663 ephyrae and scyphistomae of *A. coerulea*. This stresses the role of the lower trophic levels in  
664 the formation of the local jellyfish blooms: they promote higher levels of scyphistomae and  
665 ephyrae survival and they boost the production of buds, leading to higher scyphistomae  
666 densities and ephyrae production. In summer (during period 2) both *A. coerulea* life stages  
667 change their diet to a mix of all sources (except small plankton for medusae). This is  
668 particularly important because it supports the peak of the bloom, following high growth rates  
669 of medusae, as well as their sexual reproduction (Fig. 11; Marques et al. 2015b). It is also  
670 during this period that scyphistomae coverage declines (Fig. 11, Marques et al. 2019). Our  
671 results suggest a potentially high intraspecific trophic competition between scyphistomae and  
672 medusae, especially during this period. Therefore, the high abundance and high predation  
673 pressure of the medusae might lead to the reduction of food availability for scyphistomae and  
674 could contribute to the reduction of their coverage. During the following dry season (i.e.,  
675 period 3), a bacteria-based food web prevails in the lagoon, with internal regeneration of  
676 nitrogen, due to the absence of terrestrial freshwater inputs in the lagoon (Chapelle et al.  
677 2000). This likely supports the peaks of microzooplankton abundance since these organisms  
678 are recognized as important bacterivorous (Rassoulzadegan and Sheldon 1986).  
679 Microzooplankton appear to have a critical role as a source of food for scyphistomae, which,  
680 in period 3, would sustain not only the noticed peak of buds production in September but also

681 the main strobilation period in November (Marques et al. 2019), i.e., the first peak of ephyrae  
682 production and the initial foundation of the subsequent jellyfish bloom in the Thau lagoon.

683

#### 684 *Limitation of the study*

685 Although stable isotope analysis is a powerful tool to assess the trophic ecology of predators,  
686 the MixSIAR results should be considered with caution. Indeed, mixing models always  
687 provide a solution but their results might not always be biologically relevant: their precision  
688 decreases with the number of introduced organic matter sources and depends greatly on the  
689 accuracy of their signatures (Dubois et al. 2007).

690 In this work, we used a turnover time of one month for both jellyfish life stages, following the  
691 results reported for *Aurelia* sp. (18 – 20 days, D’Ambra et al. 2014). If inaccurate, this might  
692 have significantly biased the MixSIAR results for each isotopic niche period because the set  
693 of organic matter source signatures matching with those of the jellyfish might be incorrect.  
694 Moreover, despite the frequency of sampling for organic matter sources during our study,  
695 some periods of the year (e.g. July – September) were less represented in the database. Given  
696 the intra-annual variability in the isotopic signatures of the plankton component, we cannot  
697 fully exclude that this sampling gap slightly biased our results.

698 The implementation of different isotopic fractionation values in the mixing models also  
699 drastically modify their final results. In our study, using the fractionation values proposed by  
700 D’Ambra et al. (2014) would result in a higher contribution of mesozooplankton to the diet in  
701 both stages of *A. coerulea*. However, the values from D’Ambra et al. (2014) are very different  
702 from those typically reported in the literature (e.g. Vander Zanden and Rasmussen 2001; Post  
703 2002), leading to unrealistic trophic levels (Fleming et al. 2015; Milisenda et al. 2018).

704 Furthermore, the temperature (which is highly variable in Thau), the feeding condition, the

705 sexual maturity (e.g. Barnes et al. 2007), and, probably, the life stage might also affect  
706 fractionation and turnover values.

707

## 708 **Conclusion**

709 Knowledge of the trophic ecology and population dynamics of jellyfish is imperative  
710 to understand the main environmental drivers of blooms. With this regard, the Thau lagoon  
711 offered an exceptional framework to study both benthic and pelagic trophic interactions and to  
712 uncover the main organic matter sources supporting key periods of the *A. coerulea* life cycle.  
713 In particular, we highlight the role of phytoplankton and microzooplankton in supporting  
714 scyphistomae survival and asexual reproduction, that of mesozooplankton and sedimentary  
715 organic matter for the growth of medusae, as well as the possible negative influence of  
716 intraspecific competition on the benthic population dynamics. Moreover, we demonstrate that  
717 the interspecific trophic competition between *A. coerulea* and the commonly cultivated oyster  
718 *C. gigas* is likely to be limited, at least in the Thau lagoon, and therefore, we advocate that *A.*  
719 *coerulea* blooms have a seemingly restricted impact on the local shellfish production.

720

721

722

723

724

725

726

727 **References:**

- 728 Anderson MJ (2017) Permutational Multivariate Analysis of Variance (PERMANOVA). In:  
729 Wiley StatsRef: Statistics Reference Online. John Wiley & Sons, Ltd, Chichester, UK,  
730 pp 1–15. doi: 10.1002/9781118445112.stat07841
- 731 Båmstedt U, Wild B, Martinussen MB (2001) Significance of food type for growth of ephyrae  
732 *Aurelia aurita* (Scyphozoa). Mar Biol 139:641–650. doi: 10.1007/s002270100623
- 733 Barnes C, Sweeting CJ, Jennings S, Barry JT, Polunin NVC (2007) Effect of temperature and  
734 ration size on carbon and nitrogen stable isotope trophic fractionation. Funct Ecol  
735 21:356–362. doi: 10.1111/j.1365-2435.2006.01224.x
- 736 Boero F, Bouillon J, Gravili C, Miglietta MP, Parsons T, Piraino S (2008) Gelatinous  
737 plankton: irregularities rule the world (sometimes). Mar Ecol Prog Ser 356:299–310. doi:  
738 10.3354/meps07368
- 739 Bonnet D, Molinero J-C, Schohn T, Daly-Yahia MN (2012) Seasonal changes in the  
740 population dynamics of *Aurelia aurita* in Thau lagoon. Cah Biol Mar 53:343–347.
- 741 Boyer S, Bouvy M, Bonnet D (2013) What triggers *Acartia* species egg production in a  
742 Mediterranean lagoon? Estuar Coast Shelf Sci 117:125–135. doi:  
743 10.1016/j.ecss.2012.11.006
- 744 Chapelle A, Ménesguen A, Deslous-Paoli J-M, Souchu P, Mazouni N, Vaquer A, Millet B  
745 (2000) Modelling nitrogen, primary production and oxygen in a Mediterranean lagoon.  
746 Impact of oysters farming and inputs from the watershed. Ecol Modell 127:161–181. doi:  
747 10.1016/S0304-3800(99)00206-9
- 748 Condon RH, Graham WM, Duarte CM, Pitt KA, Lucas CH, Haddock SHD, Sutherland KR,  
749 Robinson KL, Dawson MN, Decker MB, Mills CE, Purcell JE, Malej A, Mianzan H,  
750 Uye S-I, Gelcich S, Madin LP (2012) Questioning the Rise of Gelatinous Zooplankton in  
751 the World’s Oceans. Bioscience 62:160–169. doi: 10.1525/bio.2012.62.2.9



752 D'Ambra I, Graham WM, Carmichael RH, Malej A, Onofri V (2013) Predation patterns and  
753 prey quality of medusae in a semi-enclosed marine lake: implications for food web  
754 energy transfer in coastal marine ecosystems. *J Plankton Res* 35:1305–1312. doi:  
755 10.1093/plankt/fbt065

756 D'Ambra I, Carmichael RH, Graham WM (2014) Determination of  $\delta^{13}\text{C}$  and  $\delta^{15}\text{N}$  and trophic  
757 fractionation in jellyfish: Implications for food web ecology. *Mar Biol* 161:473–480. doi:  
758 10.1007/s00227-013-2345-y

759 Dabiri JO, Colin SP, Costello JH, Gharib M (2005) Flow patterns generated by oblate  
760 medusan jellyfish: field measurements and laboratory analyses. *J Exp Biol* 208:1257 LP  
761 – 1265. doi: 10.1242/jeb.01519

762 Dawson MN, Martin DL (2001) Geographic variation and ecological adaptation in *Aurelia*  
763 *aurita* (Scyphozoa, Semaestomeae): some implications from molecular phylogenetics.  
764 *Hydrobiologia* 451:259–273. doi: <https://doi.org/10.1023/A:1011869215330>

765 Dierking J, Morat F, Letourneur Y, Harmelin-Vivien M (2012) Fingerprints of lagoonal life:  
766 Migration of the marine flatfish *Solea solea* assessed by stable isotopes and otolith  
767 microchemistry. *Estuar Coast Shelf Sci* 104–105:23–32. doi: 10.1016/j.ecss.2011.03.018

768 Dubois S, Orvain F, Marin-Léal JC, Ropert M, Lefebvre S (2007) Small-scale spatial  
769 variability of food partitioning between cultivated oysters and associated suspension-  
770 feeding species, as revealed by stable isotopes. *Mar Ecol Prog Ser* 336:151–160. doi:  
771 10.3354/meps336151

772 Dubois SF, Colombo F (2014) How picky can you be? Temporal variations in trophic niches  
773 of co-occurring suspension-feeding species. *Food Webs* 1:1–9. doi:  
774 10.1016/j.fooweb.2014.07.001

775 Dupuy C, Vaquer A, Lam-Höai T, Rougier C, Mazouni N, Lautier J, Collos Y, Le Gall S  
776 (2000) Feeding rate of the oyster *Crassostrea gigas* in a natural planktonic community of

777 the Mediterranean Thau Lagoon. *Mar Ecol Prog Ser* 205:171–184. doi:  
778 10.3354/meps205171

779 Escalas A, Ferraton F, Paillon C, Vidy G, Carcaillet F, Salen-Picard C, Le Loc’h F, Richard  
780 P, Darnaude AM (2015) Spatial variations in dietary organic matter sources modulate the  
781 size and condition of fish juveniles in temperate lagoon nursery sites. *Estuar Coast Shelf*  
782 *Sci* 152:78–90. doi: 10.1016/j.ecss.2014.11.021

783 Fleming NEC, Harrod C, Newton J, Houghton JDR (2015) Not all jellyfish are equal: isotopic  
784 evidence for inter- and intraspecific variation in jellyfish trophic ecology. *PeerJ* 3:e1110.  
785 doi: 10.7717/peerj.1110

786 Fouilland E, Trottet A, Bancon-Montigny C, Bouvy M, Le Floc’h E, Gonzalez J-L, Hatey E,  
787 Mas S, Mostajir B, Nougier J, Pecqueur D, Rochelle-Newall E, Rodier C, Roques C,  
788 Salles C, Tournoud M-G, Vidussi F (2012) Impact of a river flash flood on microbial  
789 carbon and nitrogen production in a Mediterranean Lagoon (Thau Lagoon, France).  
790 *Estuar Coast Shelf Sci* 113:192–204. doi: 10.1016/j.ecss.2012.08.004

791 Frazer TK, Ross RM, Quetin LB, Montoya JP (1997) Turnover of carbon and nitrogen during  
792 growth of larval krill, *Euphausia superba* Dana: a stable isotope approach. *J Exp Mar*  
793 *Bio Ecol* 212:259–275. doi: 10.1016/S0022-0981(96)02740-2

794 Han C-H, Uye S-I (2010) Combined effects of food supply and temperature on asexual  
795 reproduction and somatic growth of polyps of the common jellyfish *Aurelia aurita* s.l.  
796 *Plankt Benthos Res* 5:98–105. doi: 10.3800/pbr.5.98

797 Hansson LJ (2006) A method for in situ estimation of prey selectivity and predation rate in  
798 large plankton, exemplified with the jellyfish *Aurelia aurita* (L.). *J Exp Mar Bio Ecol*  
799 328:113–126. doi: 10.1016/j.jembe.2005.07.002

800 Huang XG, Huang B, Zeng Y, Li SX (2015) Effect of dinoflagellates and diatoms on the  
801 feeding response and survival of *Aurelia* sp. polyps. *Hydrobiologia* 754:179–188. doi:

802 10.1007/s10750-014-2023-1

803 Hubot N, Lucas CH, Piraino S (2017) Environmental control of asexual reproduction and  
804 somatic growth of *Aurelia* spp. (Cnidaria, Scyphozoa) polyps from the Adriatic Sea.  
805 PLoS One 12:e0178482. doi: 10.1371/journal.pone.0178482

806 Ikeda H, Mizota C, Uye S-I (2017) Bioenergetic characterization in *Aurelia aurita* (Cnidaria:  
807 Scyphozoa) polyps and application to natural polyp populations. Mar Ecol Prog Ser  
808 568:87–100. doi: 10.3354/meps12055

809 Ishii H, Båmstedt U (1998) Food regulation of growth and maturation in a natural population  
810 of *Aurelia aurita* (L.). J Plankton Res 20:805–816. doi: 10.1093/plankt/20.5.805

811 Ishii H, Tanaka F (2001) Food and feeding of *Aurelia aurita* in Tokyo Bay with an analysis of  
812 stomach contents and a measurement of digestion times. In: Purcell JE, Graham WM,  
813 Dumont HJ (eds) Jellyfish Blooms: Ecological and Societal Importance. Developments  
814 in Hydrobiology, vol 155, Springer Netherlands, Dordrecht, pp 311–320. doi:  
815 10.1007/978-94-010-0722-1\_26

816 Jackson AL, Inger R, Parnell AC, Bearhop S (2011) Comparing isotopic niche widths among  
817 and within communities: SIBER - Stable Isotope Bayesian Ellipses in R. J Anim Ecol  
818 80:595–602. doi: 10.1111/j.1365-2656.2011.01806.x

819 Jaïne AK (2010) Data clustering: 50 years beyond K-means Pattern Recognit Lett 31:651-  
820 666. 10.1016/j.patrec.2009.09.011.

821 Javidpour J, Cipriano-Maack AN, Mittermayr A, Dierking J (2016) Temporal dietary shift in  
822 jellyfish revealed by stable isotope analysis. Mar Biol 163:112. doi: 10.1007/s00227-  
823 016-2892-0

824 Kamiyama T (2013) Planktonic ciliates as food for the scyphozoan *Aurelia aurita* (s.l.):  
825 Effects on asexual reproduction of the polyp stage. J Exp Mar Bio Ecol 445:21–28. doi:  
826 10.1016/j.jembe.2013.03.018

827 Kassambara A, Mundt F (2017) factoextra: Extract and Visualize the Results of Multivariate  
828 Data Analyses. 1–74. R package version 1.0.5

829 Layman CA, Araujo MS, Boucek R, Hammerschlag-Peyer CM, Harrison E, Jud ZR, Matich  
830 P, Rosenblatt AE, Vaudo JJ, Yeager LA, Post DM, Bearhop S (2012) Applying stable  
831 isotopes to examine food-web structure: an overview of analytical tools. Biol Rev  
832 87:545–562. doi: 10.1111/j.1469-185X.2011.00208.x

833 Lo WT, Chen IL (2008) Population succession and feeding of scyphomedusae, *Aurelia aurita*,  
834 in a eutrophic tropical lagoon in Taiwan. Estuar Coast Shelf Sci 76:227–238. doi:  
835 10.1016/j.ecss.2007.07.015

836 Lucas CH (1994) Biochemical composition of *Aurelia aurita* in relation to age and sexual  
837 maturity. J Exp Mar Bio Ecol 183:179–192. doi: 10.1016/0022-0981(94)90086-8

838 Lucas CH (2001) Reproduction and life history strategies of the common jellyfish, *Aurelia*  
839 *aurita*, in relation to its ambient environment. In: Purcell JE, Graham WM, Dumont HJ  
840 (eds) Jellyfish Blooms: Ecological and Societal Importance. Developments in  
841 Hydrobiology, vol 155, Springer Netherlands, Dordrecht, pp 229–246doi: 10.1007/978-  
842 94-010-0722-1\_19

843 Lucas CH, Hirst AG, Williams JA (1997) Plankton Dynamics and *Aurelia aurita* Production  
844 in Two Contrasting Ecosystems: Comparisons and Consequences. Estuar Coast Shelf Sci  
845 45:209–219. doi: 10.1006/ecss.1996.0173

846 Marques R, Cantou M, Soriano S, Molinero J-C, Bonnet D (2015a) Mapping distribution and  
847 habitats of *Aurelia* sp. polyps in Thau lagoon, north-western Mediterranean sea (France).  
848 Mar Biol 162:1441–1449. doi: 10.1007/s00227-015-2680-2

849 Marques R, Albouy-Boyer S, Delpy F, Carré C, Le Floc'H É, Roques C, Molinero J-C,  
850 Bonnet D (2015b) Pelagic population dynamics of *Aurelia* sp. in French Mediterranean  
851 lagoons. J Plankton Res 37:1019–1035. doi: 10.1093/plankt/fbv059

852 Marques R, Darnaude AM, Schiariti A, Tremblay Y, Molinero J-C, Soriano S, Hatey E,  
853 Colantoni S, Bonnet D (2019) Dynamics and asexual reproduction of the jellyfish  
854 *Aurelia coerulea* benthic life stage in the Thau lagoon (northwestern Mediterranean).  
855 Mar Biol 166:74. doi: 10.1007/s00227-019-3522-4

856 Martinez Arbizu P (2019) pairwiseAdonis: Pairwise multilevel comparison using adonis. R  
857 package, version 0.0.1.

858 Martinussen MB, Båmstedt U (2001) Digestion rate in relation to temperature of two  
859 gelatinous planktonic predators. Sarsia 86:21–35. doi:  
860 10.1080/00364827.2001.10420458

861 Milisenda G, Rossi S, Vizzini S, Fuentes VL, Purcell JE, Tilves U, Piraino S (2018) Seasonal  
862 variability of diet and trophic level of the gelatinous predator *Pelagia noctiluca*  
863 (Scyphozoa). Sci Rep 8:12140. doi: 10.1038/s41598-018-30474-x

864 Millet B, Cecchi P (1992) Wind-induced hydrodynamic control of the phytoplankton biomass  
865 in a lagoon ecosystem. Limnol Oceanogr 37:140–146. doi: 10.4319/lo.1992.37.1.0140

866 Mills C (2001) Are population increasing globally in response to changing ocean conditions?  
867 Hydrobiologia 451:55–68. doi: <https://doi.org/10.1023/A:1011888006302>

868 Mongrue R, Vanhoutte-Brunier A, Fiandrino A, Valette F, Ballé-Béganton J, Pérez Agúndez  
869 JA, Gallai N, Derolez V, Roussel S, Lample M, Laugier T (2013) Why, how, and how  
870 far should microbiological contamination in a coastal zone be mitigated? An application  
871 of the systems approach to the Thau lagoon (France). J Environ Manage 118:55–71. doi:  
872 10.1016/j.jenvman.2012.12.038

873 Morais P, Dias E, Cruz J, Chainho P, Angélico MM, Costa JL, Barbosa AB, Teodósio MA  
874 (2017) Allochthonous-derived organic matter subsidizes the food sources of estuarine  
875 jellyfish. J Plankton Res 39:870–877. doi: 10.1093/plankt/fbx049

876 Nixon SW (1995) Coastal marine eutrophication: A definition, social causes, and future

877 concerns. *Ophelia* 41:199–219. doi: 10.1080/00785236.1995.10422044

878 Oksanen J, Blanchet FG, Friendly M, Kindt R, Legendre P, Mcglinn D, Minchin PR, O’Hara  
879 RB, Simpson GL, Solymos P, Stevens MHH, Szoecs E, Wagner H (2019) *Vegan*:  
880 *Community Ecology Package*. R package, version 2.5-4

881 Östman C (1997) Abundance, feeding behaviour and nematocysts of scyphopolyps (Cnidaria)  
882 and nematocysts in their predator, the nudibranch *Coryphella verrucosa* (Mollusca). In:  
883 Naumov AD, Hummel H, Sukhotin AA, Ryland JS (eds) *Interactions and Adaptation*  
884 *Strategies of Marine Organisms*. Springer Netherlands, Dordrecht, pp 21–28

885 Pernet F, Malet N, Pastoureaud A, Vaquer A, Quéré C, Dubroca L (2012) Marine diatoms  
886 sustain growth of bivalves in a Mediterranean lagoon. *J Sea Res* 68:20–32. doi:  
887 10.1016/j.seares.2011.11.004

888 Perrin J-L, Tournoud M-G (2009) Hydrological processes controlling flow generation in a  
889 small Mediterranean catchment under karstic influence. *Hydrol Sci J* 54:1125–1140. doi:  
890 10.1623/hysj.54.6.1125

891 Pinnegar JK, Polunin NVC (1999) Differential fractionation of  $\delta^{13}\text{C}$  and  $\delta^{15}\text{N}$  among fish  
892 tissues: implications for the study of trophic interactions. *Funct Ecol* 13:225–231. doi:  
893 10.1046/j.1365-2435.1999.00301.x

894 Pitt KA, Connolly RM, Meziane T (2009) Stable isotope and fatty acid tracers in energy and  
895 nutrient studies of jellyfish: A review. *Hydrobiologia* 616:119–132. doi:  
896 10.1007/s10750-008-9581-z

897 Plus M, La Jeunesse I, Bouraoui F, Zaldívar J-M, Chapelle A, Lazure P (2006) Modelling  
898 water discharges and nitrogen inputs into a Mediterranean lagoon: Impact on the primary  
899 production. *Ecological Modelling* 193:69–89. doi:10.1016/j.ecolmodel.2005.07.037

900 Post DM (2002) Using stable isotopes to estimate trophic position: models, methos, and  
901 assumptions. *Ecology* 83:703–718. doi: Doi 10.2307/3071875

902 Post DM, Layman CA, Arrington DA, Takimoto G, Quattrochi J, Montaña CG (2007) Getting  
903 to the fat of the matter: Models, methods and assumptions for dealing with lipids in  
904 stable isotope analyses. *Oecologia* 152:179–189. doi: 10.1007/s00442-006-0630-x

905 Purcell JE (2012) Jellyfish and Ctenophore Blooms Coincide with Human Proliferations and  
906 Environmental Perturbations. *Ann Rev Mar Sci* 4:209–235. doi: 10.1146/annurev-  
907 marine-120709-142751

908 Rassoulzadegan F, Sheldon RW (1986) Predator-prey interactions of nanozooplankton and  
909 bacteria in an oligotrophic marine environment. *Limnol Oceanogr* 31:1010–1029. doi:  
910 10.4319/lo.1986.31.5.1010

911 Stock BC, Semmens BX (2016) MixSIAR GUI User Manual. Version 3.1 1–42. doi:  
912 10.5281/zenodo.47719

913 Syväranta J, Rautio M (2010) Zooplankton, lipids and stable isotopes: importance of seasonal,  
914 latitudinal, and taxonomic differences. *Can J Fish Aquat Sci* 67:1721–1729. doi:  
915 10.1139/F10-091

916 Turk V, Lučić D, Flander-Putrlje V, Malej A (2008) Feeding of *Aurelia* sp. (Scyphozoa) and  
917 links to the microbial food web. *Mar Ecol* 29:495–505. doi: 10.1111/j.1439-  
918 0485.2008.00250.x

919 Utermöhl H (1958) Zur Vervollkommnung der quantitativen Phytoplankton-Methodik. *SIL*  
920 *Commun* 1953-1996 9:1–38. doi: 10.1080/05384680.1958.11904091

921 Wang Y-T, Zheng S, Sun S, Zhang F (2015) Effect of temperature and food type on asexual  
922 reproduction in *Aurelia* sp.1 polyps. *Hydrobiologia* 754:169–178. doi: 10.1007/s10750-  
923 014-2020-4

924 Yokoyama H, Tamaki A, Harada K, Shimoda K, Koyama K, Ishihi Y (2005) Variability of  
925 diet-tissue isotopic fractionation in estuarine macrobenthos. *Mar Ecol Prog Ser* 296:115–  
926 128. doi: 10.3354/meps296115

927 Vander Zanden MJ, Rasmussen JB (2001) Variation in  $\delta^{15}\text{N}$  and  $\delta^{13}\text{C}$  trophic fractionation:  
928 Implications for aquatic food web studies. *Limnol Oceanogr* 46:2061–2066. doi:  
929 10.4319/lo.2001.46.8.2061

930 Zheng S, Sun X, Wang Y, Sun S (2015) Significance of different microalgal species for  
931 growth of moon jellyfish ephyrae, *Aurelia* sp.1. *J Ocean Univ China* 14:823–828. doi:  
932 10.1007/s11802-015-2775-x

933 Zuur AF, Ieno EN, Walker NJ, Saveliev AA, Smith GM (2009) *Mixed Effects Models and*  
934 *Extensions in Ecology with R*. Springer New York

935

936

937

938

939



940 **Acknowledgment:**

941 We would like to thank Solenn Soriano, Nicolas Nouguier, and Remy Valdes for their  
942 technical support during SCUBA dives and fieldwork. We also thank Sandrine Crochemore  
943 and Sébastien Colantoni for their assistance during laboratory samples preparation. We thank  
944 Simon Julien from *huitres-bouzigues.com* for providing the cultivated oyster samples.  
945 Plankton diversity and abundance data are part of a long-term monitoring program on  
946 microbial communities in the Thau lagoon funded by *Observatoire des Sciences de l'Univers*  
947 *OREME* (OSU-OREME). Data are available on  
948 ([https://data.oreme.org/plankton/plankton\\_thau\\_home](https://data.oreme.org/plankton/plankton_thau_home)). The laboratory analysis of samples to  
949 determine stable isotope signatures was performed at the Stable Isotope Facility at the  
950 University of California, Davis, USA. The authors declare that they have no conflict of  
951 interests.

952 **Tables**

953 Table 1: Frequency of occurrence (FO), index of relative importance (IRI) and mean  
 954 abundance of prey items found in *A. coerulea* medusae gut contents during the period of its  
 955 presence in the Thau lagoon. Numbers in parenthesis are the number of medusae with prey  
 956 items analyzed.

Prey	FO (%)			IRI (%)			Abundance ( $\pm$ SD) (ind.medusae <sup>-1</sup> )		
	Apr (5)	May (9)	Jun (8)	Apr (5)	May (9)	Jun (8)	Apr (5)	May (9)	Jun (8)
<b>Phytoplankton</b>	20.0	33.3	0.0	3.4	5.6	0.0	1.0 (2.2)	1.0 (1.8)	0.0 (0.0)
<b>Microzooplankton</b>	60.0	55.6	0.0	7.5	12.5	0.0	2.2 (3.8)	2.2 (3.4)	0.0 (0.0)
<b>Mesozooplankton (total)</b>	80.0	88.9	100	89.1	81.9	100	26.2 (35.4)	14.6 (13.4)	10.3 (18.3)
- <i>Copepods</i>	40.0	66.7	87.5	34.7	21.9	46.3	10.2 (20.1)	3.9 (5.7)	4.8 (9.9)
- <i>Nauplii (copepods and cirripeds)</i>	60.0	88.9	62.5	4.8	31.3	41.5	1.4 (2.1)	5.6 (8.5)	4.3 (7.8)
- <i>Other crustaceans</i>	20.0	55.6	50.0	0.7	10.0	8.5	0.2 (0.4)	1.8 (3.5)	0.9 (1.1)
- <i>Non-crustaceans</i>	60.0	66.7	25.0	49.0	18.8	3.7	14.4 (20.9)	3.3 (4.5)	0.4 (0.7)

957

958

959 Table 2: Parameters of the generalized linear models used to assess correlations between the  
 960 benthic population dynamics variables (scyphistomae coverage and scyphistomae producing  
 961 buds) with the abundance  $[\ln(x+1)]$  of phytoplankton (cell L<sup>-1</sup>), microzooplankton (cell L<sup>-1</sup>)  
 962 and mesozooplankton (ind m<sup>-3</sup>).

	Estimate	Std. Error	t value	p-value
<b>Scyphistomae coverage (%)</b>				
(Intercept)	-0.17	0.07	-2.46	0.03
Phytoplankton	0.02	0.01	2.97	<b>0.01</b>
Microzooplankton	0.01	0.01	2.10	0.05
Mesozooplankton	0.00	0.00	0.02	0.98
<b>Scyphistomae producing buds (%)</b>				
(Intercept)	-3.82	0.35	-10.95	< <b>0.01</b>
Phytoplankton	-0.01	0.03	-0.47	0.64
Microzooplankton	0.26	0.03	10.19	< <b>0.01</b>
Mesozooplankton	0.00	0.02	-0.09	0.93

963

964

965 Table 3: Stable  $\delta^{13}\text{C}$  and  $\delta^{15}\text{N}$  isotope signatures (mean  $\pm$  SD) of *A. coerulea* and organic  
 966 matter sources used in MixSIAR model for each isotopic niche period. Sources A are the  
 967 values of organic matter sources used for scyphistomae models, including all data, while  
 968 Sources B are the values of organic matter sources collected from February to May, used for  
 969 medusae models. *n* is the number of samples used to calculate each mean. SP: small plankton;  
 970 Mesoz.: mesozooplankton; SOM: sedimentary organic matter.

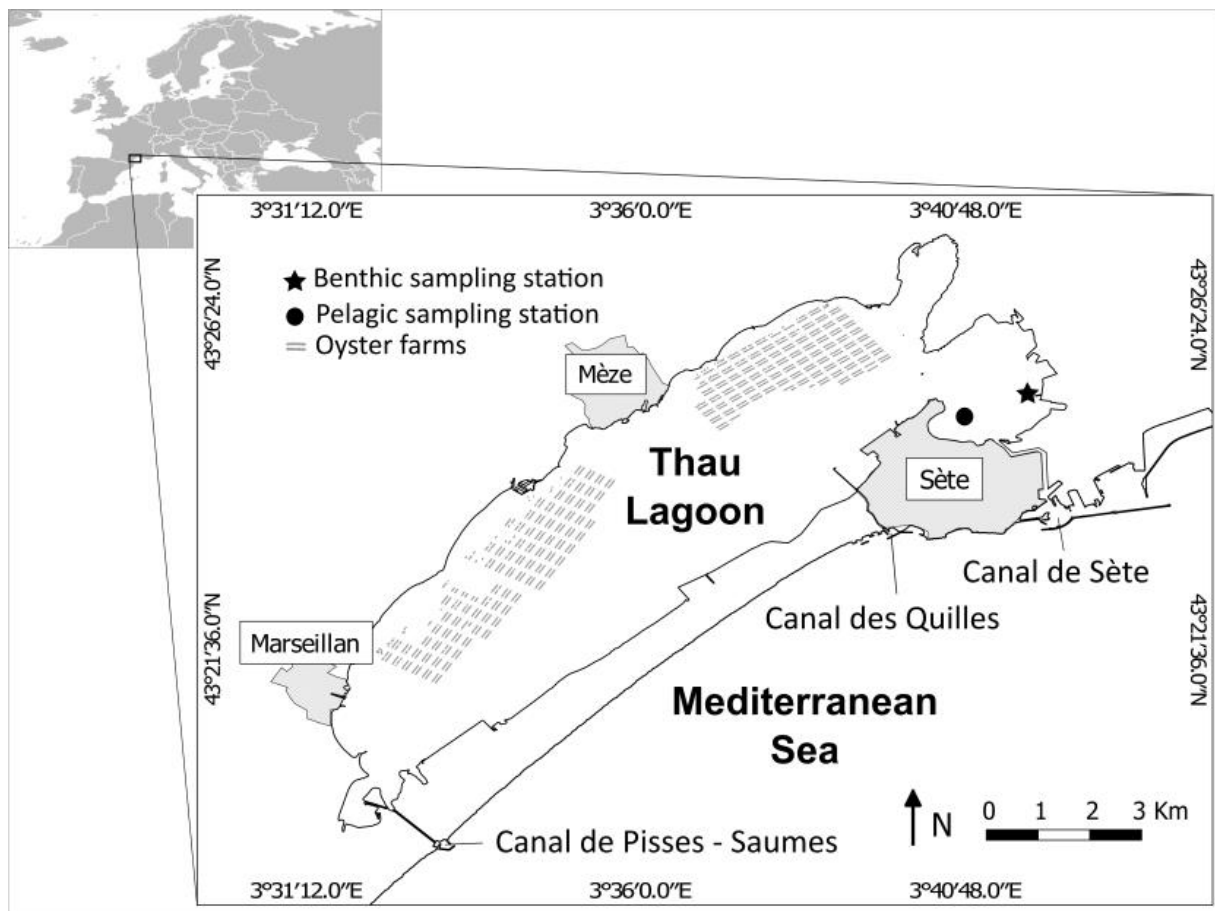
	Period 1			Period 2			Period 3		
	$\delta^{13}\text{C}$ ( $\pm$ SD) ‰	$\delta^{15}\text{N}$ ( $\pm$ SD) ‰	<i>n</i>	$\delta^{13}\text{C}$ ( $\pm$ SD) ‰	$\delta^{15}\text{N}$ ( $\pm$ SD) ‰	<i>n</i>	$\delta^{13}\text{C}$ ( $\pm$ SD) ‰	$\delta^{15}\text{N}$ ( $\pm$ SD) ‰	<i>n</i>
Scyphistomae	-22.8 (0.4)	8.0 (0.5)	18	-19.3 (0.2)	9.0 (0.1)	9	-21.1 (0.3)	8.5 (0.4)	9
Medusae	-23.4 (0.7)	8.1 (0.3)	13	-19.4 (0.5)	8.9 (0.3)	7			
<b>Sources A</b>									
SP	-22.1 (2.0)	6.5 (0.3)	18	-20.6 (0.8)	6.2 (0.7)	22	-21.0 (0.9)	6.7 (0.3)	6
Mesoz.	-22.9 (0.9)	8.0 (0.4)	9	-19.2 (0.7)	7.4 (0.3)	12	-20.1 (0.1)	7.5 (0.0)	3
SOM	-20.2 (0.9)	5.5 (0.3)	6	-20.6 (0.1)	5.4 (0.2)	6	-20.7 (0.0)	5.3 (0.0)	2
<b>Sources B</b>									
SP	-23.3 (0.9)	6.4 (0.3)	12	-20.9 (0.5)	5.8 (0.3)	15			
Mesoz.	-23.4 (0.3)	8.2 (0.2)	6	-18.8 (0.2)	7.3 (0.3)	9			
SOM	-18.9 (0.0)	5.8 (0.1)	2	-20.5 (0.0)	5.6 (0.0)	2			

971

972

973 **Figures**

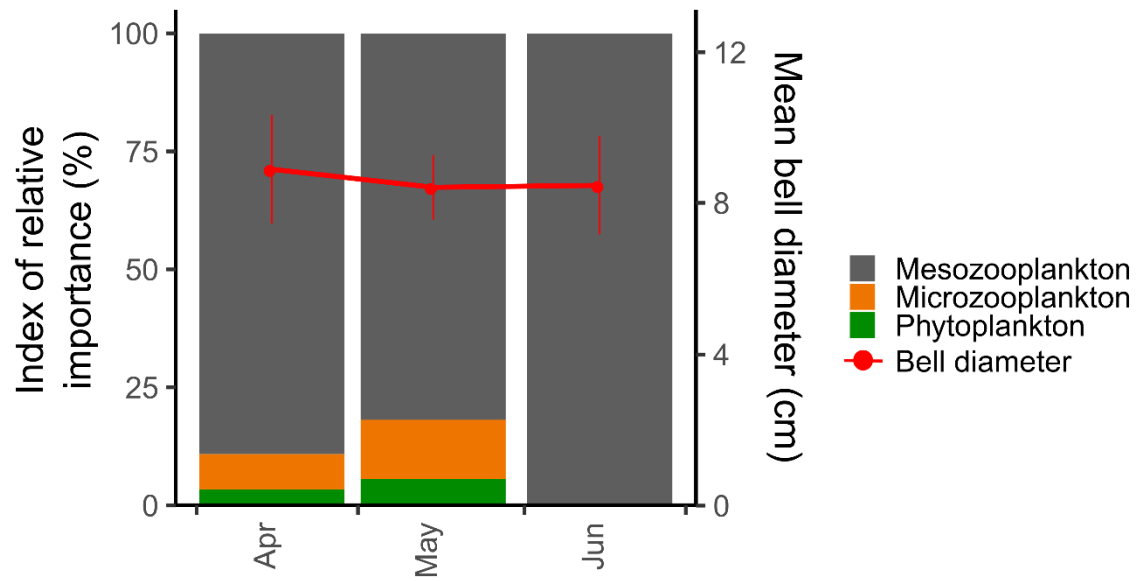
974



975

976 Fig. 1: Map of the Thau lagoon showing the location of the benthic (star) and pelagic (dot)  
977 sampling stations for this study. Shaded areas represent urban zones and grey points represent  
978 oyster farms.

979



980

981 Fig. 2: Index of relative importance of the three main prey groups found in the guts of *A.*

982 *coerulea* medusae and the bell diameter of all individuals collected for gut content analysis.

983

984

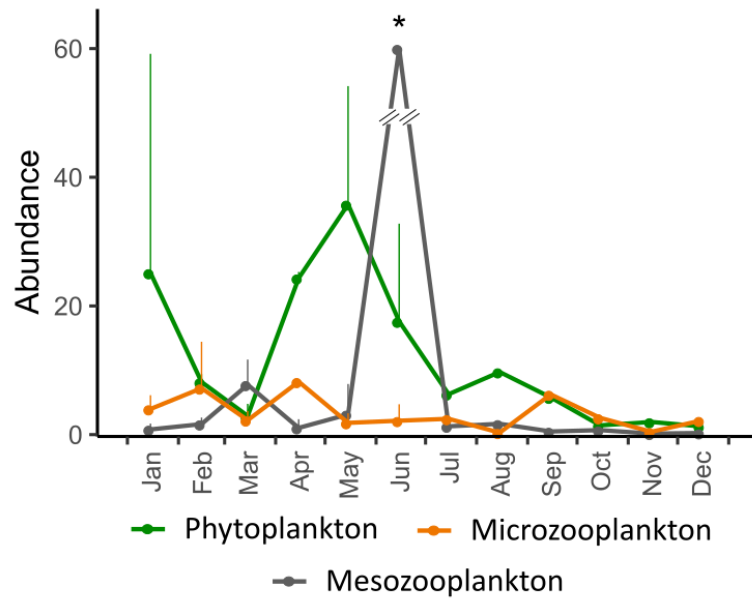
985

986

987

988

989



990

991 Fig. 3: Temporal variability of phytoplankton ( $\times 10^3 \text{ cell L}^{-1}$ ), microzooplankton ( $\times 10^3 \text{ cell L}^{-1}$ ), and mesozooplankton ( $\times 10^3 \text{ ind m}^{-3}$ ) abundance collected in the Thau lagoon during the  
 992 study period. All values represent monthly mean  $\pm$  SD. In June 2017 (\*), the mean ( $\pm$  SD) of  
 993 mesozooplankton abundance was  $90,895 \pm 107,072 \text{ ind m}^{-3}$ .  
 994

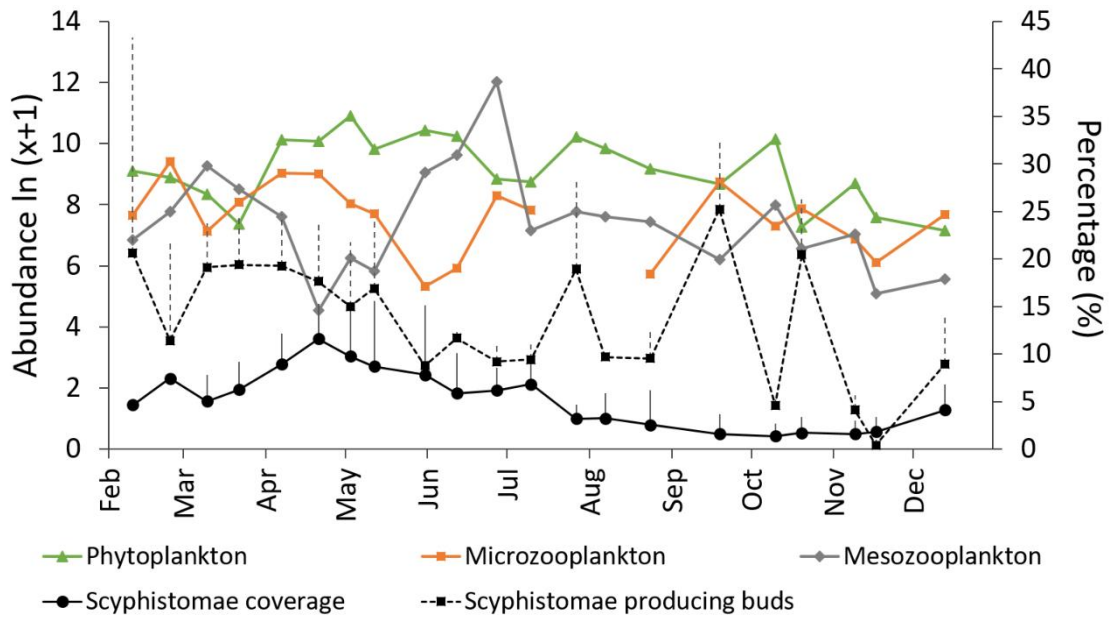
995

996

997

998

999



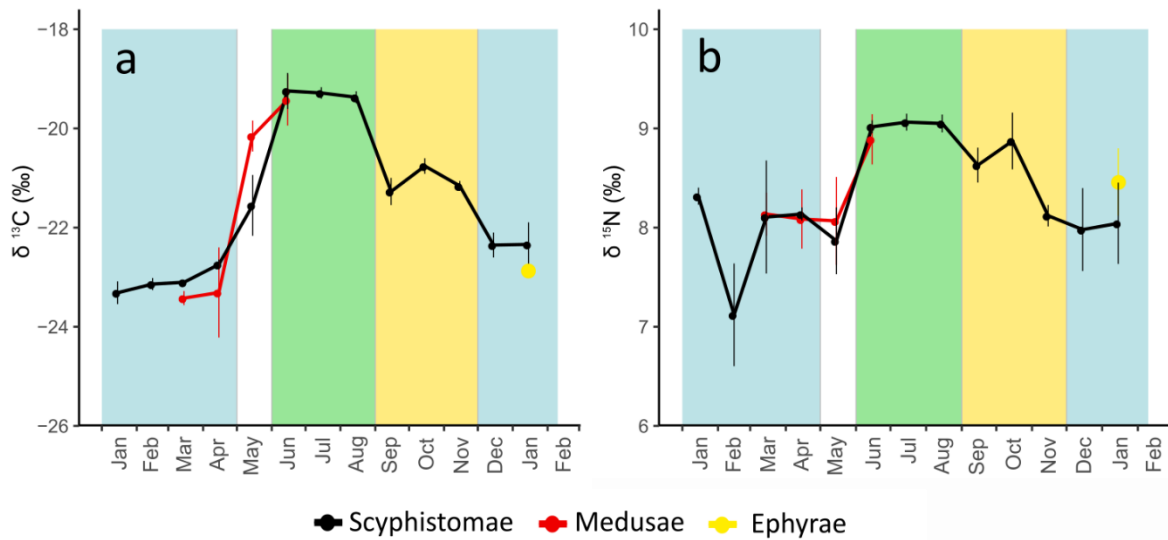
1000

1001 Fig. 4: Temporal variability of the *A. coerulea* benthic population dynamics and the  
 1002 abundance of plankton in the Thau lagoon during the study period (adapted from Marques et  
 1003 al. 2019). Black lines represent the percentage of scyphistomae coverage (i.e., an indicator of  
 1004 population size) and the percentage of the scyphistomae producing buds. Each point  
 1005 represents replicate means and vertical lines are SD (see Marques et al 2019 for further  
 1006 information). Coloured lines represent the non-averaged abundance (after logarithmic  
 1007 transformation) of phytoplankton ( $\text{cell L}^{-1}$ ), microzooplankton ( $\text{cell L}^{-1}$ ), and  
 1008 mesozooplankton ( $\text{ind m}^{-3}$ ).

1009

1010





1011

1012 Fig. 5: Temporal variability of  $\delta^{13}\text{C}$  (a) and  $\delta^{15}\text{N}$  (b) of *A. coerulea* scyphistomae, medusae,  
 1013 and ephyrae in Thau. All values represent monthly means  $\pm$  SD. Background colours  
 1014 represent the different isotopic niche periods (periods 1, 2, and 3 in blue, green, and yellow,  
 1015 respectively; see Fig.6). May represents a transitional period and it was not included in any  
 1016 isotopic niche period.

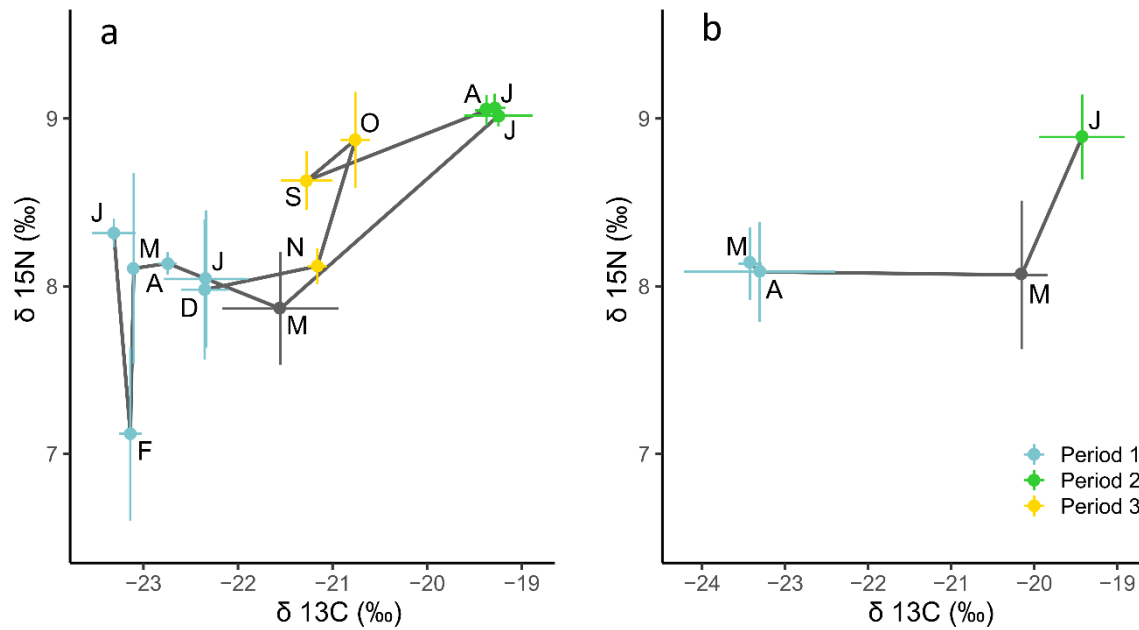
1017

1018

1019

1020

1021

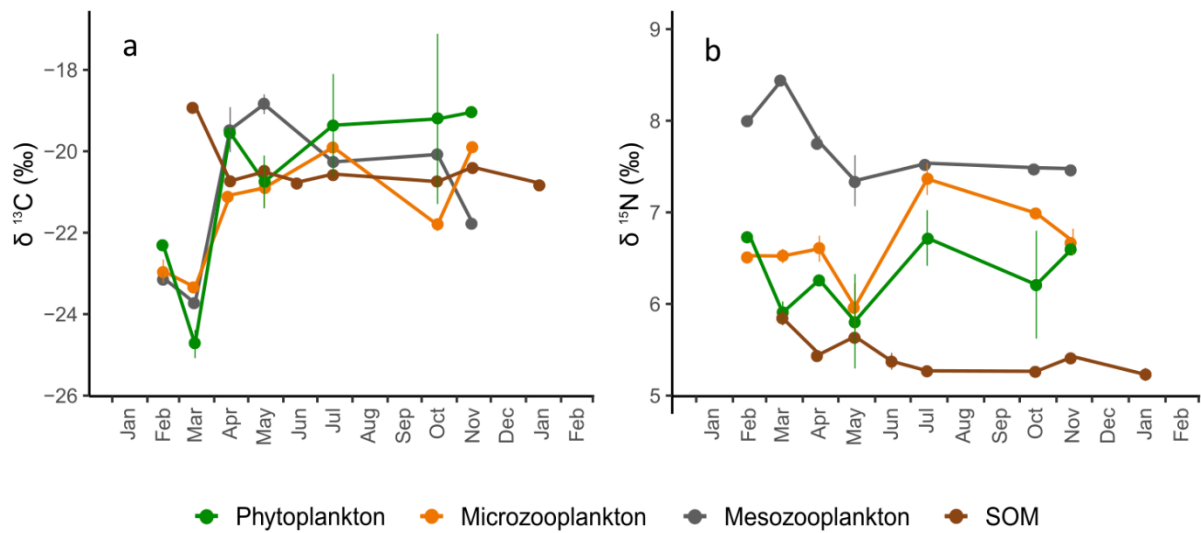


1022

1023 Fig. 6: Time trajectory of the evolution of the isotope signature, averaged by month, from *A.*  
 1024 *coerulea* scyphistomae (a) and medusae (b). Letters represent months (from January 2017 to  
 1025 January 2018). Coloured points represent isotopic niche periods defined after cluster analysis:  
 1026 period 1 is from January to April 2017 and from December 2017 to January 2018; period 2 is  
 1027 from June to August 2017 and period 3 is from September to November 2017. May represents  
 1028 the transition between periods 1 and 2 and was therefore not included in any isotopic niche  
 1029 period.

1030

1031



1032

1033 Fig. 7: Monthly variability of the  $\delta^{13}\text{C}$  (a) and  $\delta^{15}\text{N}$  (b) of the organic matter sources collected  
 1034 in this study. SOM: sedimentary organic matter.

1035

1036

1037

1038

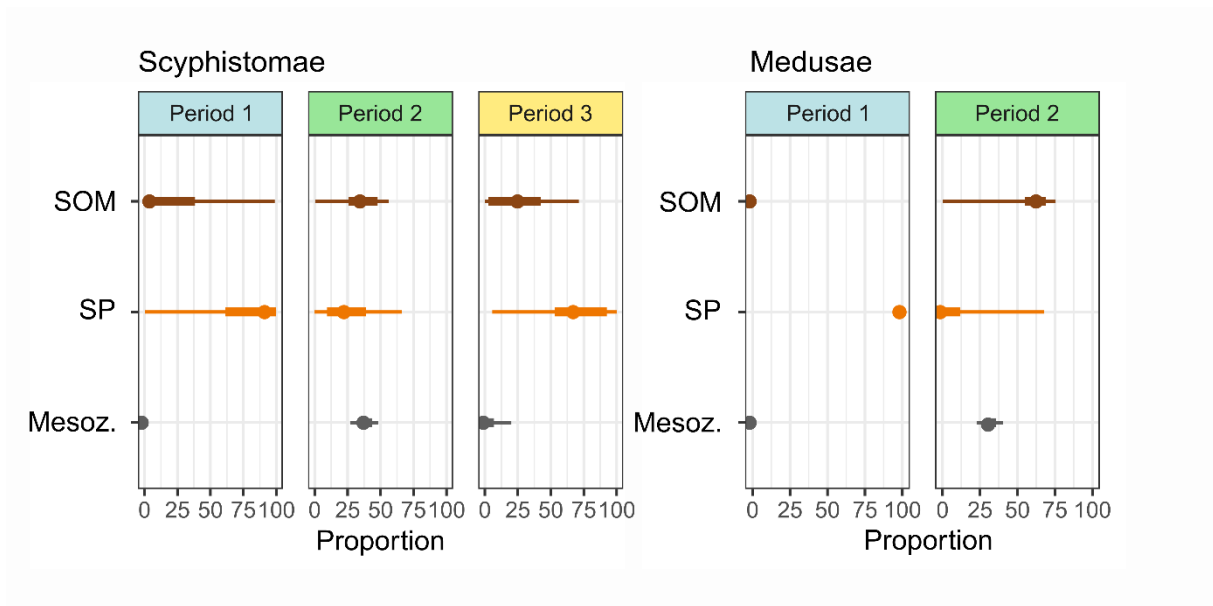
1039

1040

1041

1042

1043

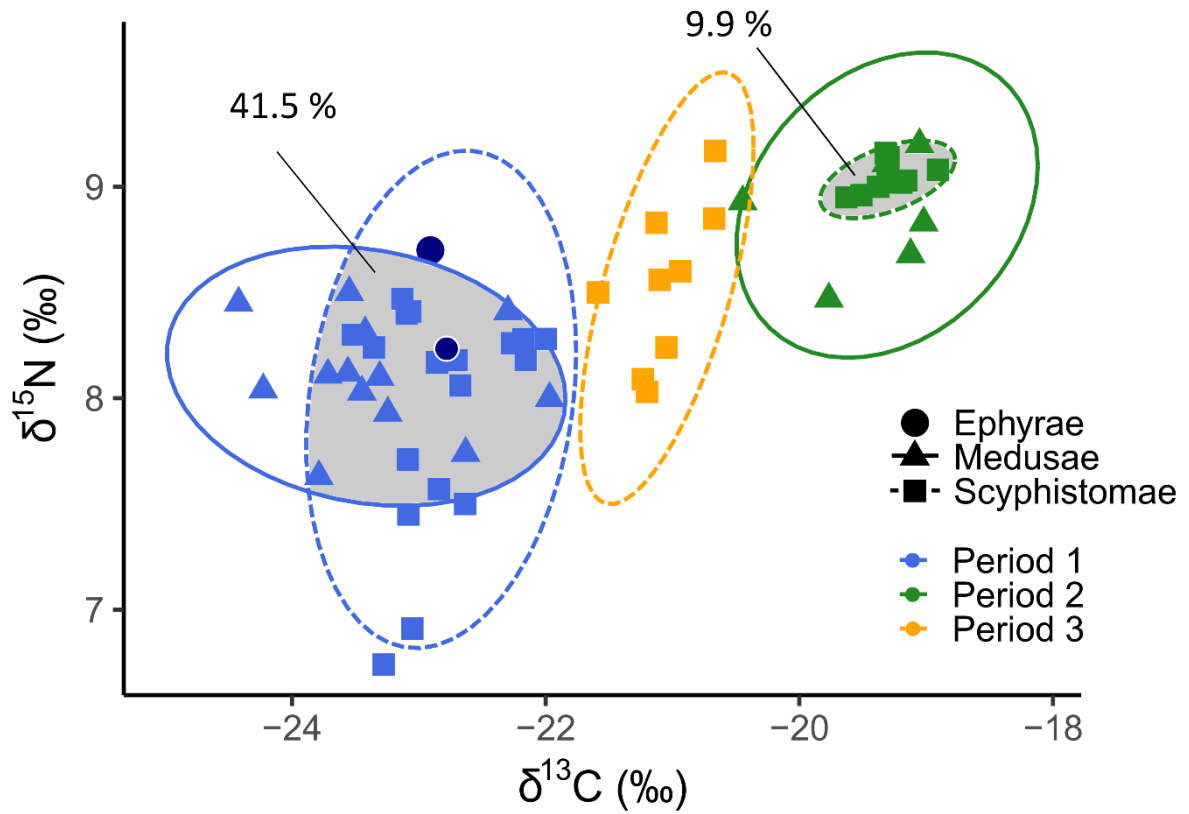


1044

1045 Fig. 8: Proportion of the contribution of each organic matter source to the diet of *A. coerulea*  
 1046 scyphistomae and medusae during the different isotopic niche periods. The proportion was  
 1047 calculated using MixSIAR mixing models. The points indicate the median and the horizontal  
 1048 bars represent 75% and 95% Bayesian credibility intervals. SOM: sedimentary organic matter,  
 1049 SP: small plankton, Mesoz.: mesozooplankton.

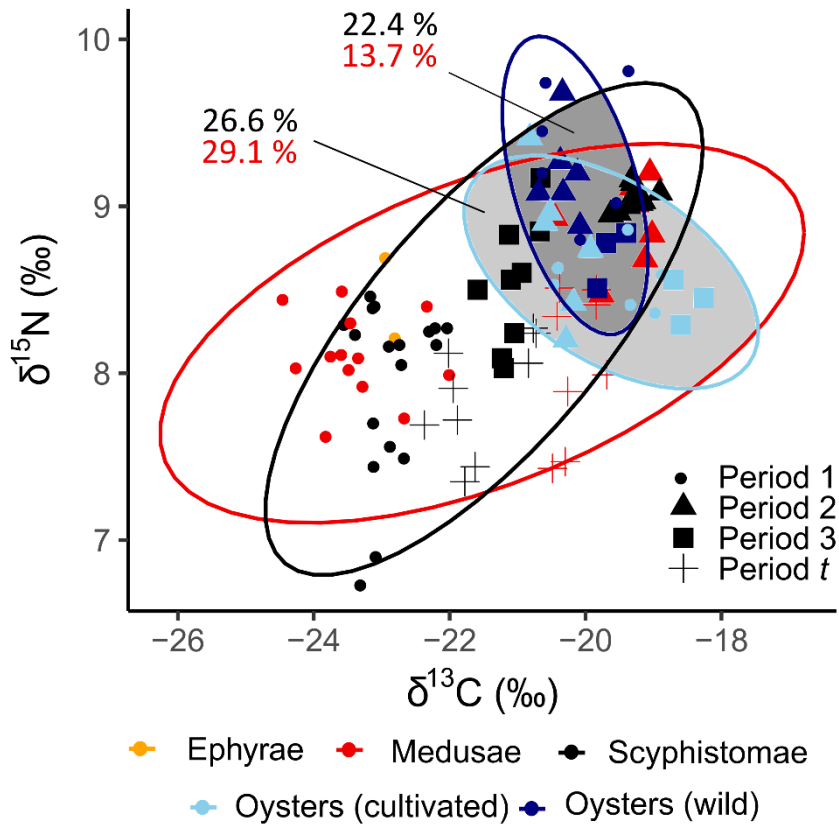
1050

1051



1052

1053 Fig. 9: Biplot of isotope values of *A. coerulea* ephyrae, medusae, and scyphistomae. Ellipses  
 1054 indicate their isotopic niche in the Thau lagoon (as 95% confidence ellipse of the bivariate  
 1055 means), during the different isotopic niche periods. Grey areas and associated values indicate  
 1056 the percentage of overlap, when observed.



1057

1058 Fig. 10: Biplot of isotope values of *A. coerulea* ephyrae, medusae, scyphistomae, and oysters

1059 (*C. gigas*). Ellipses indicate their isotopic niche in the Thau lagoon, considering the whole

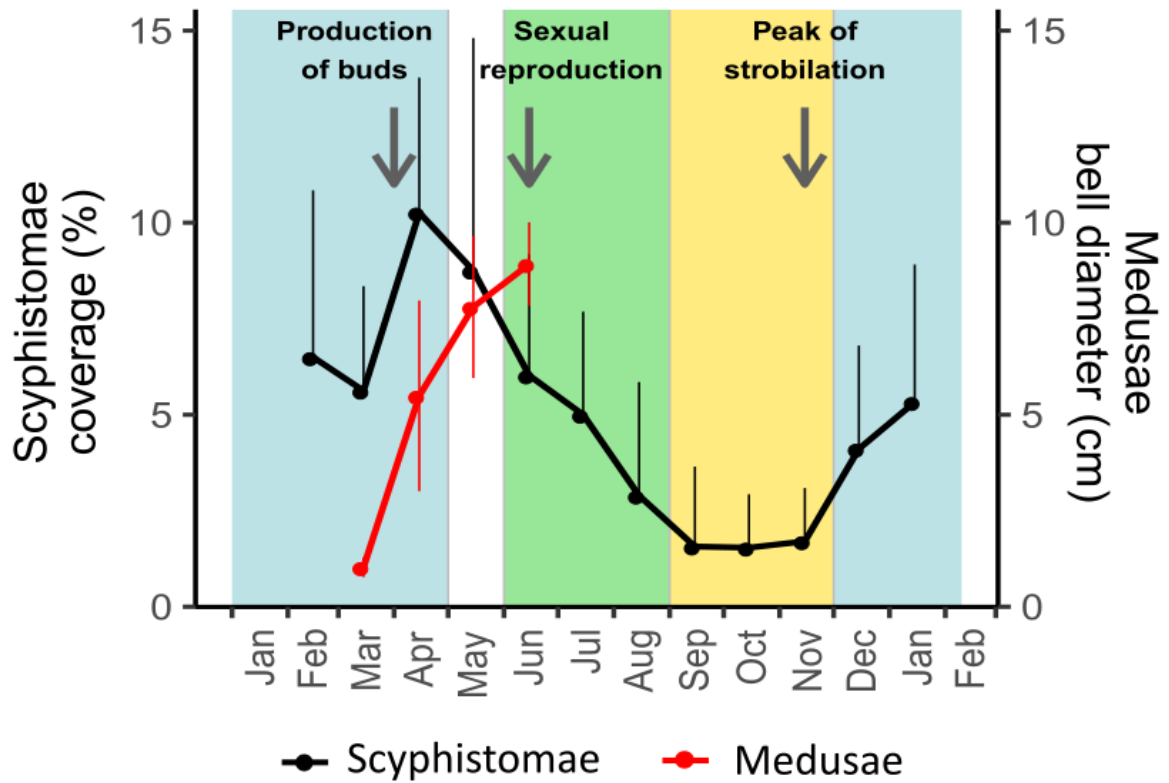
1060 study period (as 95% confidence ellipse of the bivariate means). Dark and light grey areas

1061 indicate niche overlap between *A. coerulea* and wild or cultivated oysters, respectively.

1062 Associated values on the graph indicate the percentage of overlap with medusae (in red) and

1063 scyphistomae (in black). The shape of points represents isotopic niche periods (period *t*:

1064 transitional period, i.e., samples collected in May).



1065

1066 Fig. 6: Scyphistomae coverage (in black, from Marques et al. 2019) and medusae bell  
 1067 diameter of the individuals collected for stable isotope analysis in this study (in red). The  
 1068 arrows indicate the main periods of sexual and asexual reproduction of *A. coerulea* (after  
 1069 Marques et al. 2015b, 2019). The background colours represent the isotopic niche periods  
 1070 (periods 1, 2, and 3 in blue, green, and yellow, respectively).

1071